POST-PRINT https://www.sciencedirect.com/science/article/pii/S2210670717314087
Sustainable Cities and Society, Volume 41, August 2018, Pages 227-241

Manuscript Details

Manuscript number	SCS_2017_1287_R2
Title	The impact of trees on street ventilation, NOx and PM2.5 concentrations across heights in Marylebone Rd street canyon, central London
Article type	Full Length Article

Abstract

This paper assesses the effects of trees (Platanus x hispanica) of different leaf area density on ventilation, NOx and PM2.5 concentrations across heights in Marylebone Rd street canyon in London (UK). Computational Fluid Dynamics steady state simulations are performed with OpenFOAM. The ventilation is evaluated through flow patterns and the analysis of the impact of trees on wind speed, turbulence kinetic energy, flow rates, mean and turbulent pollutant exchanges.. Results show that the effects of trees are local. For parallel winds planting new trees is positive since flow channelling and turbulence distribute the pollutant over the height which is removed by both mean flow and turbulent fluctuations through the roof. Both areas close and far from the trees within the road have a beneficial effect, with pedestrian average concentration reductions up to 18% due to aerodynamic effects. For perpendicular winds recirculation zones diminish the dispersion of pollutants and the introduction of trees has an additional negative effect with local average concentration increase up to 108% close to trees. Overall, the positive deposition effects are larger for increased LAD and for perpendicular winds may counterbalance the negative aerodynamic effects at locations close to trees.

Keywords	Urban vegetation; deposition; air quality; OpenFOAM; ventilation
Taxonomy	Natural Ventilation, Air Pollution Modeling, Green City, Urban Vegetation Impact

Corresponding Author	Riccardo Buccolieri
Corresponding Author's Institution	University of Salento
Order of Authors	Riccardo Buccolieri, Antoine Jeanjean, Elisa Gatto, Roland J. Leigh

Suggested reviewers	Mats Sandberg, Kevin Ka-Lun Lau, pietro salizzoni, Raffaele Vasaturo, Jose Luis Santiago, Chun-Ho Liu, Christof Gromke

The impact of trees on street ventilation, NO_x and $PM_{2.5}$ concentrations across heights in Marylebone Rd street canyon, central London

Abstract

This paper assesses the effects of trees (*Platanus x hispanica*) of different leaf area density on ventilation, NO_x and $PM_{2.5}$ concentrations across heights in Marylebone Rd street canyon in London (UK). Computational Fluid Dynamics steady state simulations are performed with OpenFOAM. The ventilation is evaluated through flow patterns and the analysis of the impact of trees on wind speed, turbulence kinetic energy, flow rates, mean and turbulent pollutant exchanges.. Results show that the effects of trees are local. For parallel winds planting new trees is positive since flow channelling and turbulence distribute the pollutant over the height which is removed by both mean flow and turbulent fluctuations through the roof. Both areas close and far from the trees within the road have a beneficial effect, with pedestrian average concentration reductions up to 18% due to aerodynamic effects. For perpendicular winds recirculation zones diminish the dispersion of pollutants and the introduction of trees has an additional negative effect with local average concentration increase up to 108% close to trees. Overall, the positive deposition effects are larger for increased LAD and for perpendicular winds may counterbalance the negative aerodynamic effects at locations close to trees.

Keywords: Urban vegetation; deposition; air quality; OpenFOAM; ventilation

1. Introduction

Urban vegetation affects flow and pollutant dispersion in several ways. Apart from ecosystem services such as micro-climate regulation, carbon sequestration, rainwater drainage, noise reduction, psychological and recreational values (see recent reviews by Gallagher et al., 2015; Janhäll, 2015; Salmond et al., 2016; Grote et al., 2016; Abhijith et al., 2017), urban vegetation, especially trees, may reduce the air exchange between the street and the atmosphere leading to increased concentrations below tree crowns (Gromke and Ruck, 2012). Plants may also release VOC (volatile organic compounds, precursor of the ozone), allergens and other pollutants, leading to changes to photochemistry and increased pollutant levels. On the other hand, leaves provide surfaces for removing pollutants through wet and dry deposition, adsorption and absorption. Local decreases of temperatures (Wang and Akbari, 2016; Kong et al., 2017) may modify the rate of chemical reactions, leading to decreased ozone concentrations (Salmond et al., 2016; Grote et al., 2016).

At local scale, it is still an open issue if the effect of trees is beneficial or not for local air quality. Field (e.g. Di Sabatino et al., 2015; Chen et al., 2015; Tong et al., 2015; Chen et al., 2016) and wind tunnel (e.g. Gromke and Ruck, 2012; Gromke et al., 2016) tests, as well as Computational Fluid Dynamics (CFD) studies (e.g. Gromke and Blocken 2015; Hong et al., 2017; Jeanjean et al., 2016, 2017; Selmi et al., 2016; Santiago et al., 2017a,b; Xue and Li, 2017) suggest that urban vegetation cannot be used as a general mitigation measure of urban air quality problems. Local effects should be analysed for each particular case by evaluating several interacting factors, such as predominant meteorology, building morphology and types/arrangements of trees. This has still prevented the development of general guidelines for planting trees in the urban environment (Gallagher et al., 2015).

Among the modelling studies, both aerodynamic and deposition effects of trees were considered within idealized and real scenarios. Aerodynamic effects were found to be more important than deposition for particulate matter (PM), even though the deposition effects have been found to be crucial depending on wind direction and deposition velocity (Vos et al., 2013; Jeanjean et al., 2016, 2017; Santiago et al., 2017a; Xue and Li, 2017).

Within this context, the impact of trees on flow, turbulence, ventilation conditions and nitrogen oxides (NO_x) and particulate matter ($PM_{2.5}$) concentrations is analysed in a real scenario. Modelling simulations were performed by the Computational Fluid Dynamics (CFD) code OpenFOAM equipped with a Reynolds-Averaged Navier-Stokes (RANS) closure. Different from previous studies in the city of Leicester using the same modelling approach (see Jeanjean et al., 2015, 2016), here a different real neighbourhood is considered, i.e. Marylebone in central London (UK). The starting point is the previous study performed by some of the authors (Jeanjean et al., 2017) who analysed the concentration levels under several meteorological conditions (wind speed and directions) and leaf area densities (LAD) of trees in the road. The innovation here is to perform new analyses by employing methods published in the literature to evaluate flow, turbulence and ventilation for this study area which is one of the busiest roads in London and where the British government has to face critical air pollution episodes.

2. Description of the study site and trees characteristics

Marylebone is located in the inner-city of central London (UK). It is characterised by major streets (such as Marylebone Rd), with smaller avenues between them. Marylebone Rd has an aspect ratio (height of buildings / width of the street) approximately equal to one (Nikolova et al., 2016). To build the 3-dimensional study site into the CFD model, buildings and roads, as well as trees located in the area, were collected.

Data for buildings and roads were taken from the topography and building height layers of Ordnance Survey, the UK Government mapping agency (OS, 2016). Along Marylebone Rd (up to 20 m away from the road), the maximum recorded building height is 33 m with a 17 m mean (standard deviation of 8 m). Across the whole modelling area (see Fig. 1), the maximum recorded building height is 63 m with a 12 m mean (standard deviation of 7 m). As the building layer includes small features such as bus stops or small objects, the minimum building heights is equal or below 1 m in both cases.

As for trees, the National Tree Map™ (NTM) Crown Polygon produced by Bluesky International Ltd was employed to represent single trees or closely grouped tree crowns (Bluesky, 2016). Being deciduous trees predominant in London (80.3 %) with respect to coniferous trees (19.7 %) (Forestry-Commission, 2013), only deciduous trees were explicitly modelled. The *Platanus x hispanica,* called "London plane", is the species mainly present in Marylebone Rd. Trees and bushes higher than 3 m were considered. A base height of 1/3 of the canopy depth was assumed (e.g. Gromke and Blocken, 2015). In the Marylebone Rd the mean height of tree crown top is 17 m and that of crown bottom is 5.7 m. The maximum canopy top height recorded in the street is of 29 m.

An overview of the study area is shown in Fig. 1. The greater number of trees is located in the Regent's park in the North East of the modelled area.

[Figure 1 about here]

3. Air quality and meteorology

3.1 Traffic data

Road emissions of NO_x and $PM_{2.5}$ for the average London vehicle fleet profile in the study area were estimated from Annual Average Daily Flows (AADF), Department for Transport (DfT, 2016). In addition to vehicle number, the DFT traffic counts provide the spread of traffic between cars, buses, motorcycles, buses and HGV which were then fed into the DEFRA (Department for Environment, Food & Rural Affairs) Emissions Factors Toolkit (version 6.0.2) to calculate NOx and $PM_{2.5}$ emissions (DEFRA, 2016). The traffic speed was set to the road speed limit of 30 mph, which provides a constant rate of emissions across Marylebone Rd. This means that the emissions used in this study are average across the whole street. Final emissions data are shown in Table 1 (see Jeanjean et al., 2017 for full details about their calculations).

[Table 1 about here]

3.2 Air quality analysis

Marylebone Rd is characterized by the passage of more than 80,000 vehicles per day, which usually lead to high pollution situations (Crosby et al., 2014). Fig. 2 shows monthly mean of NO_x and $PM_{2.5}$ concentrations in 2014 obtained from the monitoring station (Automatic Urban and Rural Network, AURN) located within the road. The annual mean value of NO_x is 330 µg m^{-3}, with a proportion of an annual mean of 94 µg m^{-3} for NO_2 well above the European threshold of 40 µg m^{-3}. Hourly NO_2 pollutant concentrations are in fact regularly above 200 µg m^{-3} hourly threshold more than 35 times a year (Charron et al., 2007). $PM_{2.5}$ annual mean value was 18 µg m^{-3} in 2014, which is under the 25 µg m^{-3} annual mean European regulation.

[Figure 2 about here]

NO_2 concentrations in Marylebone Rd have decreased by 1 to 6 % annually between 2010 and 2014, whereas NO_x concentrations have increased by 5% per year during the same period, showing that the introduction of new technologies or traffic conditions affected NO_x and NO_2 in a different way (Font, 2015). In the wider City of London, meeting the annual mean value of 40 µg m^{-3} for NO_2 remains a challenge. $PM_{2.5}$ concentrations have decreased in

Marylebone Rd between 2010 and 2014 by around 1% per year, similar trend in $PM_{2.5}$ concentrations decrease was observed for the other London monitoring stations (Font, 2015).

3.3 Meteorological analysis

Wind data used here refer to the year 2014 and were taken from the London City Airport weather station (EGLC, available at https://www.wunderground.com), which is about 15 km far (on the west side) of the study area. The temporal resolution of the data was 30 min and the wind direction accuracy was 10°. The average wind speed was equal to 4.3 m s^{-1} and the prevalent wind direction was South-West. The prevailing South-West wind directions in London are found to be consistent over the years, as shown by the 2013 and 2015 wind roses (Fig. 3). The annual mean wind speed was also similar in 2013 (4.2 m s^{-1}) and 2015 (4.7 m s^{-1}).

[Figure 3 about here]

4. Description of the cases and parameters investigated

4.1 Summary of previous analyses

The starting point of the present paper is the concentration analyses performed in the same area by Jeanjean et al. (2017). They evaluated aerodynamic and deposition effects of trees on NO_x and $PM_{2.5}$ concentrations at the monitoring station (AURN) positioned close to a group of trees in the Marylebone Rd and at pedestrian level. Results of their study are summarized below:

- at the monitoring station trees led to concentration increases of 7% in spring/autumn and 7.5% in summer (on average for the typical wind speed of 5 m s^{-1} and under several wind directions, i.e. perpendicular, parallel and oblique, in 2014). The aerodynamic effects were thus found to be similar during the seasons and deposition effects were 4 times lower. The calculation of aerodynamic effects corresponded to the difference between an empty street canyon (baseline scenario) and a street canyon filled with trees. The second scenario was modelled to account for the addition of trees which modify the flow (Eq. 13) and have therefore impacts on the dispersion of pollutants. For the calculation of deposition, a third scenario is run by modelling a sink term in the trees crown areas in addition to their aerodynamic effects (Eq. 14). The deposition effects of trees were then calculated as the difference between the second and third scenario. Note that all these calculations were made at a single wind direction and wind speed (specific wind condition). More deposition was found in summer than in spring and autumn due to a larger LAD. However, for winds parallel to Marylebone Rd, the aerodynamic effects decreased street concentrations and the effectiveness in altering concentrations was greater at lower wind speeds since little turbulent dispersion occurred due to inhibited mixing (aerodynamic effects), and more time was left for the suspended particles to deposit on leaves (deposition effect);

- instead, the effect of trees averaged over the pedestrian level for several wind directions was positive, with a 0.7% reduction of concentrations due to aerodynamic effects in summer, and an additional 4.6% reduction via deposition. This reduction was due to prevailing winds parallel to the street canyon which produced strong decrease, even though other wind directions produced increased concentrations. This shows that results found for the whole street are different from those found for a single point (monitoring station), confirming that any evaluation of the effects of trees should be done case by case.

4.2 Extension of the analysis to flow, turbulence and ventilation

Here the work is extended by assessing the effects of trees on mean flow, turbulence and ventilation. Specifically:

- concentrations, already analysed in Jeanjean et al. (2017) in terms of mean values within the whole Marylebone Rd., as well as velocity and turbulence, are here re-analysed across heights in the road and at specific hotspots. This will allow us to gain information at several positions, far and close to group of trees, and at several floor heights;
- the ventilation is analysed by flow rate and pollutant fluxes due to mean flow and turbulent fluctuations to clarify the relative contribution of mean flow and turbulence on pollutant exchange.

Two wind speeds are considered, i.e. 3 m s^{-1} and 5 m s^{-1}, the first leading to the greater effects of trees on pollutant concentrations, the latter being the average speed in 2014. As for wind directions, two parallel (60° and 240°) and two perpendicular (180° and 330°) directions are chosen, the parallel directions leading to strongest beneficial reduction of concentrations in the canyon (best scenarios), the perpendicular directions leading to strongest increase (worst scenarios). Leaf-free trees (typical of winter season, referred to as empty street or CB), trees with half-grown leaves (spring/autumn, referred to as CT1) and trees with fully grown leaves (summer, referred to as CT2) are investigated. Please note that CT1 and CT2 considered trees with different LAD and thus porosity (see Subsection 4.2 for details). The cases investigated are summarized in Table 2.

[Table 2 about here]

The ventilation across the Marylebone Rd is evaluated by calculating flow rates and mean and turbulent pollutant fluxes through the road openings. Flow rates are calculated as follows (Buccolieri et al., 2010; 2015):

$$q = \iint_A (\vec{V} \cdot \vec{n}) dA \qquad (\mathrm{m^3\ s^{-1}}) \qquad (1)$$

where $\vec{V}$ is the velocity vector and $\vec{n}$ is the normal unit vector to street opening of area (A) (which corresponds to the empty space between two adjacent buildings; alternatively, lateral ends and top roof of the road) . The flow rate is defined positive for air entering the street, negative for air leaving the street. The vertical flow rate is indicated by an arrow at the centre of the road. As an example, Fig. 4 shows the areas used for calculating flow rates and the nomenclature employed (subsection 5.1). Note that flow rates through empty spaces between adjacent buildings ("buildings empty spaces" hereinafter) have not been directly calculated due to the difficulty in defining such areas, however an estimation has been done since the sum of all flow rates through all the street openings (i.e. the sum of air entering and leaving the road) has to be null.

[Figure 4 about here]

At street openings both mean flows and turbulent fluctuations are calculated as they may contribute to pollutant dispersion. The pollutant fluxes due to mean flow (F_m) and turbulent fluctuations (Ft) are defined as (Fernando, 2012; Hang et al., 2012):

$$F_m = (\vec{V} \cdot \vec{n}) C(k,l) \qquad (\mathrm{mg\ s^{-1}\ m^{-2}}) \qquad (2)$$

$$F_t = -K_c \frac{\partial C(k,l)}{\partial n} \qquad (\mathrm{mg\ s^{-1}\ m^{-2}}) \qquad (3)$$

where $C(k,l)$ (mg m^{-3}) is the scalar concentration of the grid cell at the k and l locations of the street opening area and K_c (m^2 s^{-1}) is the turbulent diffusivity of pollutant. The spatially-averaged pollutant fluxes at street openings due to mean flow (FA_m) and turbulent fluctuations (FA_t) are:

$$FA_m = \iint_A F_m dA \quad (\text{mg s}^{-1}) \tag{4}$$

$$FA_t = \iint_A F_t dA \quad (\text{mg s}^{-1}) \tag{5}$$

The pollutant flux is defined positive for pollutant entering the street and negative for pollutant leaving the street.

Finally, to evaluate the impact of trees across heights, flow, turbulence and concentration are further evaluated through the analysis of profiles and contours of concentration C^* (mg m^{-3}), mean velocity U (m s^{-1}), its vertical component Uz (m s^{-1}) (or vertical velocity) and turbulent kinetic energy TKE (m^2 s^{-2}) for the cases tree *vs* tree-free as follows:

$$\Delta C^*(z) = \sum_{ij} \frac{[C_{tree}(i,j,z)] - [C_{notree}(i,j,z)]}{C_0(z)} \times 100 \quad (\%) \tag{6}$$

$$\Delta U(z) = \sum_{ij} [(U_{tree}(i,j,z)] - U_{notree}(i,j,z)] \quad (\text{m s}^{-1}) \tag{7}$$

$$\Delta Uz(z) = \sum_{ij} [(Uz_{tree}(i,j,z)] - Uz_{notree}(i,j,z)] \quad (\text{m s}^{-1}) \tag{8}$$

$$\Delta TKE(z) = \sum_{ij} [TKE_{tree}(i,j,z)] - TKE_{notree}(i,j,z)] \quad (\text{m}^2\text{ s}^{-2}) \tag{9}$$

where z is the height (m), $C_0(z)$ is the averaged scalar concentration of the tree-free case at z=1 m (mg m^{-3}) in the canyon, [$C_{tree}(i,j,z)$] is the scalar concentration of the grid cell at the i and j locations in the canyon for the case with trees (similar for U, Uz and TKE) and [$C_{notree}(i,j,z)$] is the scalar concentration of the grid cell for the tree-free case. The sum over the i and j corresponds to a sum of points sampled on a regular 2 x 2 m across the whole Marylebone Rd canyon (see Fig. 6 and Fig. 10) using an interpolation scheme for point values ("pointMVC" Mean Value Coordinates). Vertical profiles of the above parameters are presented to evaluate the global influence of trees by averaging over the whole Marylebone Rd (subsection 5.2). Urban background concentrations were added to C_0 to account for other sources than local road emission. The urban background was calculated depending on the season and wind directions (see Jeanjean et al., 2017).

5. CFD modelling

The specification of CFD simulations set-up used in this work is presented in Jeanjean et al., 2017. Here further details of the area and trees are provided.

5.1 Flow and pollutant modelling set-up

Steady-state incompressible isothermal simulations were performed using the CFD code OpenFOAM (Open Field Operation and Manipulation), an open source software platform (www.openfoam.com), with the RANS standard k–ε closure model (Launder and Spalding, 1974). Governing equations were discretized with second order upwind scheme. Mesh and computational domain were chosen based on best practice guidelines. Specifically, lateral boundaries of the domain were placed about 15 Hmax (Hmax=63 m) far from the study area, while the top was 8 Hmax. The mesh was made of about 4 million hexahedral cells, with a minimum cell size of 0.5 m in the vertical direction close to the ground and 1.25 m along the X and Y axis for buildings, trees and roads. More than 10 cells were present across the main street canyon. The expansion ratio between two consecutive cells in the regions of high gradient was kept below 1.3 (Fig. 5).

[Figure 5 about here]

Single inlet and outlet conditions were used, while the top of the domain was a symmetry plane. At the inlet, the mean velocity, the turbulent kinetic energy (TKE) and the turbulent dissipation rate (ε) were set as follows:

$$U = \frac{u_*}{\kappa} ln\left(\frac{z + z_0}{z_0}\right) \qquad (\mathrm{m\ s^{-1}}) \qquad (10)$$

$$TKE = \frac{u_*^2}{\sqrt{C_\mu}} \qquad (\mathrm{m^{-2}\ s^{-2}}) \qquad (11)$$

$$\varepsilon = \frac{u_*^3}{\kappa \cdot z}\left(1 - \frac{z}{\delta}\right) \ (\mathrm{m^{-2}\ s^{-3}}) \qquad (12)$$

where U is the fluid velocity (ms^{-1}), u_* the frictional velocity (ms^{-1}), κ the von Karman constant, z the vertical coordinate (m), δ the boundary layer depth (m) and z_0 the surface roughness (m). The atmospheric boundary layer was set to reach the wind speed at a height of 10 m to match wind measurement, using z_0 = 0.10 m which corresponds to sparse, large obstacles. As for gaseous pollutant dispersion modelling set-up, the advection diffusion (AD) module was used with a turbulent Schmidt number Sc_t of 0.5 (Jeanjean et al., 2017). The source was placed at ground level and corresponded to the road cells up to 1.5 m height.

Emissions rates are those summarized in subsection 3.1.

The residual convergence of 10^{-5} was set for the flow field variables, 10^{-4} for the pressure and 10^{-6} for the scalar dispersion (pollutant).

5.2 Modelling the effects of trees

Both aerodynamic and deposition effects of trees were modelled. A sink of momentum has been considered to model the aerodynamics effects, i.e. trees were modelled following Green (1992) and Liu et al. (1996) by adding the sink (*S*) variable to the cells occupied by the trees:

$$S = - c_d LAD(\frac{1}{2}\rho U u_i) \quad (\text{Pa m}^{-1}) \tag{13}$$

where C_d = 0.25 is the sectional drag for vegetation (dimensionless), LAD is the Leaf Area Density ($m^2 m^{-3}$), u_i is the appropriate wind velocity component (m s^{-1}), U is the wind speed (m s^{-1}). For the summer season, an average LAD of 1.6 m^2 m^{-3} was set (Di Sabatino et al., 2015). In spring and autumn (growth and fall of leaves, respectively), the LAD was set to 1.06 $m^2 m^{-3}$. Finally, in winter the LAD was 0 $m^2 m^{-3}$.

In the literature, aerodynamic effects have been also parametrized by adding source and sink terms in turbulence kinetic energy and turbulence dissipation energy equations (e.g. Amorim et al. 2013; Santiago et al. 2013; Gromke and Blocken 2015; Krayenhoff et al. 2015; Santiago et al., 2017a,b,c). There are few studies comparing the different parameterizations (see Buccolieri et al., 2018 for a review). For example, Santiago et al. (2017a) using parameterizations of turbulent kinetic energy and dissipation sink/source terms for vegetation did not obtained much better fit of experimental concentrations than using only the sink of momentum. On the other hand, validation exercises using CODASC wind-tunnel experiments (Gromke et al., 2008; Buccolieri et al., 2011; Jeanjean et al., 2015) have modelled the vegetation only taking into account the sink of momentum and applying RANS models, obtaining a good agreement with measured concentrations. These exercises include also the same OpenFOAM model employed here (Jeanjean et al., 2015), which has been further validated against NOx and $PM_{2.5}$ concentrations obtained from a monitoring station in Marylebone Rd (Jeanjean et al., 2017) and which constitutes the starting point of the present paper (see subsection 3.4).

As for the deposition effects of trees, the following change in particle concentration via deposition (*ΔC*) has been added as sink term to take into account the deposition of $PM_{2.5}$ on trees (Vranckx et al., 2015):

$$\Delta C = C_0 \cdot LAD \cdot V_d \quad (\mathrm{g\ m^{-3}\ s^{-1}}) \tag{14}$$

where C_0 is the initial particle concentration (g m^{-3}) and V_d is the deposition velocity (m s^{-1}) taken equal to 0.64 cm s^{-1} (Pugh et al., 2012).

It should be noted that Eq. (14) works for homogenous vegetation surfaces which is not the fulfilled in real situations. Strictly speaking, leaves are aligned in different orientation to the wind flows which is not included in the above parameterization. However, this is a challenge in CFD models and currently not feasible to model individual leaves which would require a model resolution of much less than 1 m. Further, this would imply the evaluation of each single tree of the street under different seasons which is also impracticable. For these reasons an average deposition velocity is used to model the whole crown area. The scientific community is moving towards a better representation of vegetation in CFD models (e.g. see the case studies of different density of leaves across the canopy in Hofman et al., 2016) as well as in wind tunnel experiments. The full variability of the real world cannot be taken into consideration in steady state CFD models, thus some assumptions are made based on the purpose of the study. Eq. 14 can then be seen as an average sink term of the trees on $PM_{2.5}$ over the whole crown area, which has been applied in several studies (e.g. Vranckx et al., 2015). The validation made in the previous paper (Jeanjean et al., 2017) against monitored data provide us with a certain confidence about the accuracy of the employed CFD set-up. Thus, here the intention is to show what happens on average in the street and provide some insights on the main mechanisms behind the concentration results presented in the previous paper.

5.3 Consideration on the employed turbulence model and validation

Here the RANS standard *k*-*ε* model has been employed. It is known that Large Eddy Simulations (LES) perform better in predicting turbulence than RANS models (Liu et al., 2015). While there are still challenges to their applications (computational time, wall boundary conditions, appropriate time-dependent inlet), steady RANS approaches have been shown to successfully predict the spatial distribution of mean velocity and concentration fields. RANS models are in fact still widely used to investigate the main feature charactering the mechanics of ventilation of street canyons and urban canopies, as recently done in the comprehensive MUST CFD-evaluation exercise within COST Action 732 (Di Sabatino et al., 2011).

Among RANS, several RANS models exist and have been employed with success in idealized and complex scenarios (Tominaga and Stathopoulos, 2009). Here the same CFD OpenFOAM-k-ε model used in previous studies (Jeanjean et al., 2015, 2016, 2017) has been employed, which makes use of the standard k-ε turbulence model. The intention here is in fact to make a further step of employing such methodology to explore the impact of trees on concentrations found in Jeanjean et al. (2017) in the same area by analysing the influence on flow, turbulence and ventilation conditions.

Literature studies found that the differences of the results between the standard k-ε and the modified k-ε models are rather small for dispersion in street canyons and building complexes, where turbulence produced by surrounding buildings is dominant (Tominaga and Stathopoulos, 2013) as happens in the present case. To further gain confidence, Jeanjean et al. (2015) and Vranckx et al. (2015) validated the OpenFOAM k-ε model used here against the CODASC wind tunnel database for flow and pollutant dispersion within an idealized street canyon with and without trees. Finally, CFD simulations employed here have been validated against monitored data in the Marylebone Rd (Jeanjean et al., 2017).

For these reasons, we are confident that the results are accurate enough to explore in detail the spatial flow and concentration distribution and the ventilations conditions.

6. Results and discussion

The primary focus is on flow patterns and street ventilation across Marylebone Rd through the analysis of flow rates and pollutant fluxes (Eqs. 1-2) and contours of velocity. Then, vertical profiles of concentration, mean velocity, vertical velocity and TKE (Eqs. 3-6) are shown to evaluate the differences trees *vs* no trees for both the whole depth of the road and at specific hotspots.

6.1 Flow patterns and ventilation over the whole Marylebone Rd

To analyse the influence of trees on street ventilation, Fig. 6 shows zoomed sketches of flow entering and leaving the road, as calculated through flow rates shown in Table 3 for the wind speed of 3 m s^{-1}, as well as contours coloured by the vertical velocity Uz. Results for the wind speed of 5 m s^{-1} have similar behaviours. We remind here that a negative flow rate indicates air leaving Marylebone Rd, while a positive value indicates air entering the street.

[Figure 6 about here]

[Table 3 about here]

To quantitatively analyse the impact, Fig. 7 further shows:

- $[(q_{inlet\mathrm{CT}} - q_{inlet\mathrm{CB}})$ x $100/q_{inlet\mathrm{CB}}]$ (%), "q_{inlet} tree impact" hereinafter, where $q_{inlet\mathrm{CT}}$ is the total (positive) flow rate at inlets in CT1 and CT2 cases and $q_{inlet\mathrm{CB}}$ is the total (positive) flow rate at inlets in the CB case (i.e. air entering the street). This allows to evaluate the percentage reduction of air entering the street due to the presence of trees (Fig. 7a);
- $[(q_{\mathrm{roof}}/q_{\mathrm{inlet}})$ x 100] (%), "q roof/inlet" hereinafter, where q_{roof} is the absolute value of the flow rate at top street roof and q_{inlet} is the total flow rate at inlets. This allows to evaluate the amount of air exiting through the street roof with respect to total air entering the street (Fig. 7b);
- $[(q_{\mathrm{down}}/q_{\mathrm{inlet}})$ x 100] (%), "q down/inlet, where q_{down} is the absolute value of the flow rate at the downstream end of the street. This allows to evaluate the amount of air exiting through the downstream end with respect to total air entering the street (Fig. 7b).

[Figure 7 about here]

Finally, to further evaluate the relative contribution of mean flow and turbulent fluctuations on pollutant exchanges trough the street openings, Table 4 shows the $PM_{2.5}$ pollutant fluxes (without deposition) and wind speed of 3 m s^{-1}.

[Table 4 about here]

Figs. 6, 7 and Tables 3,4 show that the ventilation pattern is similar with and without trees, i.e. the air enters or exits the Marylebone Rd similarly for all the cases investigated (CB, CT1 and CT2). However, significant differences are found between parallel and perpendicular approaching winds as discussed below.

6.1.1 Parallel winds

For WD=60° and WD=240° the air enters the street through the upstream end and the buildings empty spaces, while it exits through the downstream end (see Fig. 4 for the nomenclature) and the top roof (Fig. 6a,b). In the presence of trees, "q_{inlet} tree impact" is negative, i.e. the ventilation at the street inlet is reduced up to 33% (CT2) for WD=60° and

23% (CT2) for WD=240° with respect to CB, since there is less air entering the street due to the blocking effects of trees which partially act as impermeable obstacles making the air rising above the upstream buildings. As expected, such blocking effect is slightly larger for CT2 than CT1 as trees are less porous and for WD=60° since more trees are located at the East end (blocking the street entrance) than at the West end (Fig. 7a).

By looking at "*q* roof/inlet" and "*q* down/inlet" shown in Fig. 7b, it can be argued that "*q* roof/inlet" increases from 69%-79% for CB (for WD=60° and 240°, respectively) to 82%-89% for CT2 (i.e. the air exits through the roof with respect to that entering through the inlet is larger in the presence of trees than in the empty street), while "*q* down/inlet" decreases from 31%-21% for CB (for WD=60° and 240°, respectively) to 18%-11% for CT2 (i.e. the air exits the street through the downstream end with respect to that entering through the inlet is lower in the presence of trees than in the empty street).

By looking at Table 4, it can be seen that mean flow across the downstream end slightly help pollutant removal and, as expected from flow rates, its effect becomes smaller in the presence of trees, with a reduction of mean pollutant exchange up to 71% with respect of the tree-free case. The major fraction of pollutant is removed out by both mean flow (*FAm*) and turbulent fluctuations (*FAt*) through the top roof, and the total roof exchange (by mean flow and turbulent fluctuations) increases in the presence of trees. The reason is that the air is blocked and forced to be vertically transported to the roof level where pollutant is removed by vertical mean flow and vertical turbulent diffusion. Further, in the presence of trees, the turbulent exchange becomes up to about 60% larger than the empty case and constitute the main mechanism for the removal of pollutants.

6.1.2 Perpendicular winds

For WD=330°, the air enters through the West and East ends and exits through the top roof. It is likely that the wind enters through the upstream buildings empty spaces and exits through the downstream ones (Fig. 6d). On the other hand, for WD=180°, being not exactly perpendicular (but oblique) to the road axis, the air enters through the West end and exits through the East as expected from the channelling of the flow along the road (Fig. 6c).

The channelling for WD=180° is qualitatively similar to parallel wind cases and thus "q_{inlet} tree impact" is negative, i.e. the ventilation at the street inlet is reduced up to 23% for CT2 with respect to CB, with low downstream exchange (i.e. the ventilation at the street outlet *q* down/inlet decreases from 11% for CB to 6% for CT2) and almost full roof exchange (i.e. "*q* roof/inlet" increases from 89% for CB to 94% for CT2). Note that for WD=180° the flow rate *q* at buildings empty spaces can be considered positive (entering air) at both street sides (in analogy with flow patterns for parallel approaching winds) and thus *q* roof/inlet and *q* down/inlet have been calculated, while for WD=330° it was not possible to guess if flow rates at both sides of buildings empty spaces were positive or negative. From Fig. 7a it can be argued that the slightly positive "q_{inlet} tree impact" (6%) is due to the interaction with trees located within the Marylebone since now air is entering the road through the minor streets.

By looking at Table 4, it can be seen that for WD=180° the major fraction of pollutant is removed out by both mean flow through the top roof. In the presence of trees, the turbulent exchanges increase up to 32% with respect to the tree-free case, but still remain less important than the mean exchange. As expected from flow rates, this behaviour is similar to the parallel winds, but the turbulent exchange is less important since the channelling flow is characterized by lower wind velocities along the street where the removal is thus dominated by mean flow. On the other hand, for WD=330° the pollutant removal is expected to occur across the downstream building empty spaces in the empty case, while the turbulent exchange through the roof becomes more important in the presence of trees (more than doubled with respect to the empty case) due to their blocking effect.

To summarize, in the presence of trees it is expected that the air exchange through the street roof is more important and constitutes the main mechanism for removing pollutants rather than the exchange through the ends of the street. This is most important under perpendicular winds, since parallel winds promote also the exchange through the downstream end due to the channelling of flow along the street.

6.2 Velocity, turbulence and concentration profiles over the whole Marylebone Rd

To explore the changes of concentration along the depth and height of the street, which is crucial for exposure of people living at highest floors, vertical profiles of horizontally-averaged values of ΔC^* (for $PM_{2.5}$) are shown in Fig. 8 for the wind speed of 3 m s^{-1}. Horizontally-averaged values are calculated at 6 different heights (horizontal planes z=1, 1.5, 5, 10, 15 and 20 m). Table 5 reports on the mean (averaged over all the depth of the canyon), the pedestrian (at z=1.5 m) and top (at z=20 m) values of ΔC^*. With a mean building height of 17 m, the chosen heights permit the exploration of changes in concentration with height up to above the mean street roof. Further, the mean height of tree crown top inside the canyon is 17 m and that of crown bottom is 5.7 m, which allows the evaluation of flow patterns below and above tree crowns. Similar results were found for the approaching wind of 5 m s^{-1} (not shown here), but with slightly lower effects.

In general, as found at pedestrian level by Jeanjean et al. (2017), independently from LAD (i.e. CT1 and CT2), Fig. 8a shows that the aerodynamic effects of trees lead to mean concentration decreases under parallel winds WD=60° and 240° (ΔC^*=-8% and -3-4%, respectively) and increase under perpendicular winds WD=180° and 330° (ΔC^*=32-36% and 6-8%, respectively) (Table 5). Note that the aerodynamic effects are similar for both $PM_{2.5}$ and NO_x since the only difference was the road emissions and the effect of deposition which occurred only for $PM_{2.5}$.

As mentioned in Ghasemian et al. (2017) increased LAD has an impact on both aerodynamic and deposition effects and can either lead to improve or deteriorate the air quality. Accordingly, here we found that larger LAD leads to larger aerodynamic effects, but LAD mostly affects the deposition by enhancing the deposition flux, especially for perpendicular winds (Fig. 8b). Specifically, the combined aerodynamic and deposition effects leads to mean ΔC^* equal to 31% (WD=180°) and -5% (WD=330°) (Table 5). It can be noted that for WD=330° mean ΔC^* from 8% under aerodynamics effects becomes -5% under the combined effects, suggesting the predominance of deposition over aerodynamic.

[Figure 8 about here]

[Table 5 about here]

To analyse in detail the mechanisms responsible of these concentration changes, Fig. 9 shows vertical profiles of horizontally-averaged values of ΔU, ΔUz and ΔTKE. Results are analysed for perpendicular and parallel winds in conjunction with ventilation analysis discussed in subsection 5.1.

[Figure 9 about here]

6.2.1 Parallel winds

Less air entering the street in the presence of trees, as shown by flow rates in Fig. 7a, does not necessarily mean that the effect of trees on pollutant dispersion is negative. In fact, in general positive effects of trees are found with concentration reductions for both CT1 and CT2 with respect to CB (Fig. 8 and Table 5).

The greater (positive) aerodynamic effects of trees on concentration occur at smaller heights (i.e. below and within crowns) (Fig. 8a), with a pedestrian percentage reduction (ΔC^* < 0) up to -16% (Table 5). We remind here that the maximum canopy top height inside the canyon is of 29 m, which justifies the reduction velocity also up at 20 m. However, even though trees have a large influence on flow (in terms of decreasing mean velocity *U*) (Fig. 9a), since the average vertical velocity *U*z is positive (see Fig. 6) for all the cases investigated at all heights, pollutant emitted at ground level is vertically transported above the street roof. The concentration decrease can thus be explained by the fact that the reduction of *Uz* ($\Delta Uz < 0$) in the presence of trees is low (and even positive for WD=240°) and the increase of *TKE* ($\Delta TKE > 0$) is large (Fig. 9b,c), confirming what found by ventilation analysis (Fig. 7b and Table 4), i.e. the air exchange through the street roof is more important and the mixing due to trees enhances the turbulent dispersion and thus diminishes the concentration levels.

It should also be noted that for WD=240° the mean concentration reduction in the presence of tree is less pronounced (-3% to -4%) than for WD=60° (-8%), on the contrary there is a slight increase at higher levels (above 10 m) up to 2% at z=20 m (see Fig. 8a and Table 5). This can be explained by the fact that in the presence of trees at WD=240° a lower downstream exchange (i.e. *q* down/inlet) and a larger roof exchange (i.e. *q* roof/inlet) (see Fig. 7) is observed, meaning that the pollutant tends to locally accumulate along the street more than the WD=60° case. $\Delta Uz > 0$ below and within crowns for WD=240° suggests that more pollutant is transported above the crowns, where the concentration in fact increases. On the other hand, for WD=60° the fact that the downstream exchange (i.e. *q* down/inlet) is more pronounced than for WD=240° implies that some pollutant is channelled along the street (Fig. 6b) and available to be locally removed through the roof (i.e. *q* roof/inlet is larger, see Fig. 7a and pollutant fluxes in Table 4) by a larger turbulent dispersion (Fig. 9c).

The deposition slightly affects the concentration levels (Fig. 8b), with a pedestrian ΔC^* up to -19% (opposite to -16% for aerodynamics effects alone) for CT2 (large LAD) (Table 5), suggesting the predominance of the aerodynamic effects. However, for WD=240°, which experienced concentration increases above tree crowns by aerodynamic effects, the deposition is able to lead to ΔC^* close to 0 at the top, indicating that even under high vertical velocity less pollutant is available to be transported above as occurs in the absence of deposition (Fig. 8a).

6.2.2 Perpendicular winds

Similar to parallel wind cases, in general the greater aerodynamic effects of trees on concentration occurs at smaller heights (i.e. below and within the crowns, Fig. 8a), but leading to pedestrian percentage increase ΔC^* ($\Delta C^* > 0$) of 26% for CT2 (large LAD) (Table 5). This may be explained by a larger influence on flow (in terms of mean velocity ΔU) below and within the crowns (Fig. 9a). The figure shows in fact that trees decrease the velocity (i.e. $\Delta U < 0$) at all heights and the larger decrease is up to the top of the average crown height. The pollutant is thus locally accumulated along the street due to recirculation zones typical of a perpendicular approaching wind case (see Fig. 6).

Fig. 8 also shows that trees affect concentrations above the crowns (positive or negative ΔC^* are found at highest levels). The maximum canopy top height of 29 m justifies the reduction of U ($\Delta U<0$) at 20 m; and being the average vertical velocity Uz positive (see Fig. 6), vertical profiles of ΔUz (Fig. 9b) shows that trees decrease also the vertical velocity (i.e. $\Delta Uz<0$) over all heights, meaning that trees increase pollution trapping (less vertical dispersion). The negative ΔUz is larger within the tree crowns (especially for CT2, large LAD), suggesting that less pollutant is transported above the crowns, thus indicating that trees have an effect also above the tree crowns. Larger negative ΔUz than the parallel wind cases and negative ΔTKE (Fig. 9b,c) (i.e. a larger vertical velocity and a lower TKE in the presence of trees with respect to the empty case) indicate that the vertical velocity mostly contributes to the concentration increases in the presence of trees shown in Fig. 8a. The pollutant locally accumulates along the street in recirculation zones and is not able to disperse by turbulence at roof level (see flow rates and pollutant fluxes and profiles in Fig. 9) leading to a concentration increase with respect to the empty street case CB (Fig. 8).

Greater deposition is observed on the side of the street where trees are present (see Fig. 10) and where the largest concentrations are located, which leads to greater deposition flux. In particular for WD=330° pedestrian ΔC^* becomes negative, i.e. -6% (opposite to 13% for aerodynamics effects alone) for CT2 (large LAD) (Table 5). For WD=180° the effect of deposition is still pronounced but not sufficient to lead to concentration decrease since this case experiences very high negative aerodynamic effects.

6.3 Pedestrian hotspots in the Marylebone Rd

To finally explore the impact of trees at pedestrian level, Fig. 10 shows concentration contours at z=1.5 m for CB and CT2 for the four wind directions. The figure shows that for parallel approaching winds the channelling of flow (see Fig. 6) distributes the pollutants along the whole street and the introduction of new trees is positive (concentration decrease) for areas close and far from trees (Fig. 10a,b). For perpendicular winds, as expected from flow patterns, in the absence of trees the concentration is larger at the leeward side, and the introduction of trees has a negative effect (concentration increase) mainly close to planted trees (Fig. 10c,d).

[Figure 10 about here]

Two representative points (hotspots of concentration) are chosen (indicated in Fig. 10) and Table 6 reports on mean, pedestrian and top values of ΔC^* along the vertical profiles (similar to results presented in Table 5, except that the values now are the actual values calculated by the model at the different heights and not the horizontally-averaged values for the whole road shown in subsection 5.2). The table shows that, on average, results are in line with those found for the whole Marylebone Rd, i.e. the aerodynamic effects were positive ($\Delta C^* < 0$) under parallel winds and negative ($\Delta C^* > 0$) under perpendicular winds due to the presence of strong recirculation regions (see Fig. 6); and the deposition is more significant under perpendicular winds close to trees, with minor effects far from trees.

Specifically, under parallel winds, at both hotspots, the mean reduction by aerodynamic effects is larger for WD=60° (up to -18%) than WD=240° (up to -9%) due to the stronger ventilation reduction of the large amount of trees present at the east end of the street (see Fig. 6 and Table 3). The highest pedestrian values of ΔC^* are -38% for WD=60° far from trees and -33% for WD=240° close to trees. As stated above, deposition has minor effects also for pedestrian values.

Under perpendicular winds, similar to parallel winds, the aerodynamic effects are also different depending on wind direction and location. The mean positive ΔC^* by aerodynamic effects is larger for WD=180° (up to 108% close to trees) than WD=330° (up to 47% far from trees). The increase far from trees is due to the obstruction of trees located far at the west of the hotspot, since the flow entering the street is channelled along the main road similar to the parallel winds cases (see Fig. 6). Close to trees the mean increase is due to the strong obstruction under perpendicular winds, even though pedestrian ΔC^* is negative for WD=180°.

As expected, the deposition is much stronger close to trees, totally counterbalancing the average increase by aerodynamic for WD=330° and reducing mean ΔC^* from 108% to 66% for WD=180°.

[Table 6 about here]

6.4 Summary of the effects of trees on concentration in the Marylebone Rd

The analysis of street ventilation and vertical profiles in the Marylebone Rd indicates that:

- trees affect wind velocity and turbulence depending on LAD and these effects depend on wind direction and are different at across heights. While trees are found to trap pollutants for perpendicular winds over the whole height of the street, for parallel winds the effects may be positive or negative at different heights, i.e. pedestrians can have advantages from the introduction of trees, while people standing at higher building floors may be subjected to an increase of pollutant concentrations especially for low LAD where the aerodynamic effects dominate over the deposition;
- the flow pattern is not qualitatively altered by the presence of trees, but the velocity is reduced, and the turbulence is increased especially for parallel winds. From a pure dynamical point of view, trees increase pollutant concentrations under perpendicular winds and decrease under parallel winds. On the other hand, deposition is greater for large LAD and may dominate over the aerodynamic effects especially for perpendicular winds, while it is not crucial for parallel winds;
- the effect of trees is strictly local. For parallel winds the flow channelling distributes the pollutants along the whole street and planting new trees is positive since turbulence dominates over the vertical velocity in distributing the pollutants over the height of the street and the main mechanism of air exchange occurs at street roof. This implies that both areas close and far from the trees within the road have a beneficial effect. On the other hand, for perpendicular winds the main mechanism of air exchange is still through the roof, but the presence of recirculation zones diminishes the dispersion of pollutants within the street and the introduction of new trees has an additional negative effect especially close to trees;
- taking in mind that the average tree crown height is similar to the average building height, the present results found for Marylebone Rd are in agreement with previous findings that, at least for perpendicular approaching winds, the vegetation above the building roof height may increase the concentration in comparison with the no vegetation case, even taking into account pollutant deposition (Santiago et al., 2017a).

It is worth underlining that this work is limited to the case study investigates here or to cases characterized by similar geometries subjected to perpendicular and parallel winds. However, results confirm previous findings that the effects of trees on pollutant concentration levels in urban areas are altered by multiple variables. In isolated street canyons, the effects of trees and hedges have been clearly evidenced and depend on street aspect ratio, wind direction, crown porosity and tree species and arrangements (Gromke et al., 2012), whereas real scenarios are complicated by the presence of surrounding buildings, asymmetric street canyons and intersections which create extra turbulence mixing leading to complex flow patterns. It is thus not obvious to evaluate a priori any action tailored to mitigate pollution levels in urban areas by the introduction of new trees (Santiago et al., 2017b).

Here we expect that since buildings surrounding the Marylebone Rd were explicitly represented, the real complexity was captured by the model and thus results found for the road can be representative of the actual situation and impact of trees in different seasons and under different meteorological conditions. Concentration contours at pedestrian level presented here could also be used to check hotspots characterized by strong recirculation zones and high concentration levels, which can be considered sensible areas for concentration monitoring in the future.

7. Conclusions

This work aims at assessing the impact of urban trees on ventilation and pollutant concentration levels within the Marylebone Rd (UK). Several scenarios have been investigated to evaluate the relative importance of both aerodynamic and deposition effects of trees of different LAD for specific meteorological conditions. Two wind speeds, one of 3 m s^{-1} leading to the greater effects of trees on pollutant concentrations, the other of 5 m s^{-1} being close the average speed in 2014 (4.3 m s^{-1}), were considered. As for wind direction, two parallel and two perpendicular directions were chosen, the first leading to strongest beneficial reduction of concentrations in the street (best scenarios), the latter leading to strongest increase (worst scenarios). Main findings confirm that negative trapping aerodynamic effects characterize the whole depth of the investigated road under perpendicular winds, but the deposition may become crucial and lead to concentration decrease, dominating over the aerodynamic effects. Positive aerodynamic effects were instead found under parallel winds, with no crucial contribution of the deposition. Such results are discussed in terms of ventilation provided by flow rates and pollutant fluxes. Further, the analysis of velocity and turbulence vertical profiles has shown that trees have different local effects across the heights and the horizontal location of the road, still suggesting that the impact of trees is particularly site-specific.

References

1. Abhijith, K.V., Kumar, P., Gallagher, J., McNabola, A., Baldauf, R., Pilla, F., Broderick, B., Di Sabatino, S., Pulvirenti, P., 2017. Air pollution abatement performances of green infrastructure in open road and built-up street canyon environments – A review.

Atmospheric Environment 162, 71-86.

2. Amorim, J. H., Rodrigues, V., Tavares, R., Valente, J., Borrego, C., 2013. CFD modelling of the aerodynamic effect of trees on urban air pollution dispersion. Science of the Total Environment 461, 541-551.
3. Bluesky, 2016. UK National Tree Map (NTM), internet database. http://www.bluesky-world.com/national-tree-map, accessed 2016-11-18.
4. Buccolieri, R., Salim, S.M., Leo, L.S., Di Sabatino, S., Chan, A., Ielpo, P., de Gennaro, G., Gromke, C., 2011. Analysis of local scale tree-atmosphere interaction on pollutant concentration in idealized street canyons and application to a real urban junction. Atmospheric Environment 45, 1702-1713.
5. Buccolieri R., Sandberg M., Di Sabatino S., 2010. City breathability and its link to pollutant concentration distribution within urban-like geometries. Atmospheric Environment 44, 1894-1903.
6. Buccolieri, R., Salizzoni, P., Soulhac, L., Garbero, V., Di Sabatino, S., 2015. The breathability of compact cities. Urban Climate 13, 73-93.
7. Buccolieri, R., Santiago, J.L., Ramos, E.R., Sanchez, B., 2018. Review on urban tree modelling in CFD simulations: aerodynamic, deposition and thermal effects. Under review: Urban Forestry & Urban Greening.
8. Charron, A., Harrison, R. M., Quincey, P., 2007. What are the sources and conditions responsible for exceedences of the 24h PM10 limit value (50μgm-3) at a heavily trafficked London site? Atmospheric Environment 41, 1960-1975.
9. Chen, X., Pei, T., Zhou, Z., Teng, M., He, L., Luo, M., Liu, X., 2015. Efficiency differences of roadside greenbelts with three configurations in removing coarse particles (PM10): A street scale investigation in Wuhan, China. Urban Forestry & Urban Greening 14, 354–360.
10. Chen, L., Liu, C., Zou, R., Yang, M., Zhan, Z., 2016. Experimental examination of effectiveness of vegetation as bio-filter of particulate matters in the urban environment. Environmental Pollution 208, 198-208.
11. Crosby, C. J., Fullen, M. A., Booth, C. A., Searle, D. E., 2014. A dynamic approach to urban road deposited sediment pollution monitoring (Marylebone Road, London, UK). Journal of Applied Geophysics 105, 10-20.
12. DEFRA, 2016. UK Department for Environment, Food & Rural Affairs Emissions Factors Toolkit (EFT), internet database. http://laqm.defra.gov.uk/review-and-assessment/tools/emissions-factors-toolkit.html, accessed 2016-11-18.

13. DfT, 2016. UK Department for Transport traffic counts, internet database. http://www.dft.gov.uk/traffic-counts/cp.php, accessed 2016-11-18.
14. Di Sabatino, S., Buccolieri, R., Pappaccogli, G., Leo, L.S., 2015. The effects of trees on micrometeorology in a real street canyon: consequences for local air quality. International Journal of Environment and Pollution 58, 100-111.
15. Fernando, H.J., 2012. Handbook of Environmental Fluid Dynamics, Two-Volume Set, CRC Press; 1 edition.
16. Font, A., Fuller, G., 2015. Roadside air quality trends in London–identifying the outliers Part. Environmental Research Group, King's College London.
17. Forestry-Commission, 2013. National Forest Inventory: standing timber volume for coniferous trees in Britain. http://www.forestry.gov.uk/pdf/FCNFI111.pdf/$FILE/FCNFI111.pdf, accessed 2016-09-08.
18. Gallagher, J., Baldauf, R., Fuller, C.H., Kumar, P., Gill, L.W., McNabola, A., 2015. Passive methods for improving air quality in the built environment: A review of porous and solid barriers. Atmospheric Environment 120, 61-70.
19. Ghasemian, M., Amini, S., Princevac, M., 2017. The influence of roadside solid and vegetation barriers on near-road air quality. Atmospheric Environment 170, 108-117.
20. Green, S.R., 1992. Modelling turbulent air flow in stand of widely-spaced trees. Phoenics J 5, 294–312.
21. Gromke, C., Buccolieri, R., Di Sabatino, S., Ruck, B., 2008. Dispersion study in a street canyon with tree planting by means of wind tunnel and numerical investigations–evaluation of CFD data with experimental data. Atmospheric Environment 42, 8640-8650.
22. Gromke, C., Blocken, B. 2015. Influence of avenue-trees on air quality at the urban neighborhood scale. Part II: Traffic pollutant concentrations at pedestrian level. Environmental Pollution, 196, 176-184.
23. Gromke, C., Jamarkattel, N., Ruck, B., 2016. Influence of roadside hedgerows on air quality in urban street canyons. Atmospheric Environment 139, 75-86.
24. Grote, R., Samson, R., Alonso, R., Amorim, J.H., Cariñanos, P., Churkina, G., Fares, S., Le Thiec, D., Niinemets, Ü., Mikkelsen, T.N., Paoletti, E., Tiwary, A., Calfapietra, C., 2016. Functional traits of urban trees in relation to their air pollution mitigation potential: A holistic discussion. Frontiers in Ecology and the Environment 14, 543-550.
25. Hang, J., Li, Y., Buccolieri, R., Sandberg, M., Di Sabatino, S., 2012. On the contribution of mean flow and turbulence to city breathability: the case of long streets with tall

buildings. Science of the Total Environment 416, 362-373.

26. Hofman, J., Bartholomeus, H., Janssen, S., Calders, K., Wuyts, K., Van Wittenberghe, S., Samson, R., 2016. Influence of tree crown characteristics on the local PM10 distribution inside an urban street canyon in Antwerp (Belgium): A model and experimental approach, Urban Forestry & Urban Greening, Volume 20, 265-276.
27. Hong, B., Lin, B., Qin, Q., 2017. Numerical investigation on the coupled effects of building-tree arrangements on fine particulate matter (PM2.5) dispersion in housing blocks. Sustainable Cities and Society 34, 358-370.
28. Janhall, S., 2015. Review on urban vegetation and particle air pollution – Deposition and dispersion. Atmospheric Environment 105, 130-137.
29. Jeanjean, A.P.R., Hinchliffe, G., McMullan, W.A., Monks, P.S., Leigh, R.J., 2015. A CFD study on the effectiveness of trees to disperse road traffic emissions at a city scale. Atmospheric Environment 120, 1-14.
30. Jeanjean, A.P.R., Monks, P.S., Leigh, R.J., 2016. Modelling the effectiveness of urban trees and grass on PM2.5 reduction via dispersion and deposition at a city scale. Atmospheric Environment 147, 1-10.
31. Jeanjean, A.P.R., Buccolieri, R., Eddy, J., Monks, P.S., Leigh, R.J., 2017. Air quality affected by trees in real street canyons: The case of Marylebone neighbourhood in central London, Urban Forestry & Urban Greening 22, 41-53.
32. Kong, L., Lau, K.K-L., Yu, C., Chen, Y., Xu, Y., Ren, C., Ng, E., 2017. Regulation of outdoor thermal comfort by trees in Hong Kong. Sustainable Cities and Society 31, 12-25.
33. Krayenhoff, E.S., Santiago, J.L., Martilli, A., Christen, A., Oke, T.R., 2015. Parametrization of drag and turbulence for urban neighbourhoods with trees. Boundary-Layer Meteorology 156, 157-189.
34. Launder, B.E., Spalding, D.B., 1974. The numerical computation of turbulent flows. Computer Methods in Applied Mechanics and Engineering 3, 269–289.
35. Liu, J., Chen, J.M., Black, T.A., Novak, M.D., 1996. E − e modelling of turbulent air flow downwind of a model forest edge. Boundary-Layer Meteorology 77, 21–44.
36. Liu, C.H. Ng, C.T. Wong, C.C.C., 2015. A theory of ventilation estimate over hypothetical urban areas. Journal of Hazardous Materials 296, 9-16.
37. Nikolova, I., MacKenzie, A. R., Cai, X., Alam, M. S., Harrison, R. M., 2016. Modelling component evaporation and composition change of traffic-induced ultrafine particles during travel from street canyon to urban background. Faraday discussions.
38. OS, 2016. Ordnance Survey: Britain Mapping Agency, internet database.

https://www.ordnancesurvey.co.uk/, accessed 2016-11-18.

39. Pugh, T.A.M., MacKenzie, A.R., Whyatt, J. D., Hewitt, C. N., 2012. Effectiveness of green infrastructure for improvement of air quality in urban street canyons. Environmental Science & Technology 46, 7692-7699.
40. Salmond, J.A., Tadaki, M., Vardoulakis, S., Arbuthnott, K., Coutts, A., Demuzere, M., Dirks, K.N., Heaviside, C., Lim, S., Macintyre, H., McInnes, R.N., Wheeler, B.W. Health and climate related ecosystem services provided by street trees in the urban environment. Environmental Health 2016, 15(Suppl 1): 36.
41. Santiago, J.L., Martin, F., Martilli, A., 2013. A computational fluid dynamic modeling approach to assess the representativeness of urban monitoring stations. Science of the Total Environment 454–455, 61–72.
42. Santiago, J.-L., Martilli, A., Martin, F., 2017a. On Dry Deposition Modelling of Atmospheric Pollutants on Vegetation at the Microscale: Application to the Impact of Street Vegetation on Air Quality. Boundary Layer Meteorology 162, 451-474.
43. Santiago, J.-L., Rivas, E., Sanchez, B., Buccolieri·, R., Martin, F., 2017b. On the influence of aerodynamics and deposition effects of street vegetation on NOx concentrations at pedestrian level: the case of Plaza de la Cruz neighborhood in Pamplona (Spain). Atmosphere 2017 8, 131.
44. Santiago, J.L., Borge, R., Martin, F., de la Paz, D., Martilli, A., Lumbreras, J., Sanchez, B., 2017c. Evaluation of a CFD-based approach to estimate pollutant distribution within a real urban canopy by means of passive samplers. Science of the Total Environment 576, 46-58.
45. Selmi, W., Weber, C., Rivière, E., Blond, N., Mehdi, L., Nowak, D. (2016). Air pollution removal by trees in public green spaces in Strasbourg city, France. Urban Forestry & Urban Greening, 17, 192-201.
46. Tominaga, Y., Stathopoulos, T., 2009. Numerical simulation of dispersion around an isolated cubic building: Comparison of various types of k-□ models. Atmospheric Environment 43, 3200-3210.
47. Tominaga, Y., Stathopoulos, T., 2013. CFD simulation of near-field pollutant dispersion in the urban environment: a review of current modeling techniques. Atmospheric Environment 79, . 716-730.
48. Tong, Z., Whitlow, T.H., MacRae, P.F., Landers, A.J., Harada, Y., 2015. Quantifying the effect of vegetation on near-road air quality using brief campaigns. Environmental Pollution 201, 141-149.

49. Vos, P. E., Maiheu, B., Vankerkom, J., Janssen, S., 2013. Improving local air quality in cities: to tree or not to tree?. Environmental pollution, 183, 113-122.

50. Vranckx, S., Vos, P., Maiheu, B., Janssen, S., 2015. Impact of trees on pollutant dispersion in street canyons: A numerical study of the annual average effects in Antwerp, Belgium. Science of the Total Environment 532, 474-483.

51. Xue, F., Li, X., 2017. The impact of roadside trees on traffic released PM10 in urban street canyon: Aerodynamic and deposition effects. Sustainable Cities and Society 30, 195-204.

52. Wang, Y., Akbari. H., 2016. The effects of street tree planting on Urban Heat Island mitigation in Montreal. Sustainable Cities and Society 27, 121-128.

Figure captions

Figure 1. (a) GoogleEarth overview and (b) 3D model of the area of interest. Source emissions for the roads are reported in Table 1 (note that residential roads are omitted in the model due to their low emissions) (adapted from Jeanjean et al., 2017).

Figure 2. Monthly mean values of NO_x and $PM_{2.5}$ (μg m^{-3}) in 2014 obtained from Marylebone monitoring station (AURN). The error bars correspond to the standard deviation from the monthly means.

Figure 3. Wind rose plots showing wind directions (°) and wind speeds during the year 2013, 2014 (reference year, from Jeanjean et al., 2017) and 2015 in central London (data: London City Airport weather station).

Figure 4. Sketch of areas of the road openings used to calculate flow rates: upstream end, downstream end, top roof and buildings empty spaces (not shown here). The case refers to the wind direction WD=60°.

Figure 5. (a) Sketch of the Marylebone Rd from GoogleEarth and (b) mesh used for CFD simulations (adapted from Jeanjean et al., 2017).

Figure 6. Flow rates (left) and contours of vertical velocity (Uz) in the whole Marylebone Rd (CB: middle; CT2: right) for approaching wind directions (a) WD=60°, (b) WD=240°, (c) WD=180° and (d) WD=330°. Dotted arrows indicate the estimated pattern of flow based on the calculation of flow rates through other areas.

Figure 7. Graphs showing the impact of trees on flow rates. (a) "q_{inlet} tree impact" indicates the percentage reduction of air entering (which is equal to that leaving) the street due to the presence of trees. (b) "q roof/inlet" indicates the amount of air exiting through the street roof with respect to total air entering the street; "q down/inlet" indicates the amount of air exiting through the downstream end with respect to total air entering the street.

Figure 8. Vertical profiles of horizontally-averaged ΔC^* for tree *vs* tree-free cases under wind speed of 3 m s^{-1} and four wind directions (WD=60°, WD=180°, WD=240°, WD=330°) within Marylebone Rd: a) aerodynamic effects (V_d=0), b) aerodynamic and deposition effects (V_d=0.64cm s^{-1}). The dashed line rectangle indicates the position of the mean tree crown, i.e. 17 m (mean height of the top) and 5.7 m (mean height of the bottom). The maximum canopy top height recorded in the street is of 29 m.

Figure 9. Vertical profiles of horizontally-averaged ΔU, ΔUz and ΔTKE for tree *vs* tree-free cases under wind speed of 3 m s^{-1} and four wind directions (WD=60°, WD=180°, WD=240°, WD=330°) within Marylebone Rd: a) aerodynamic effects (V_d=0), b) aerodynamic and deposition effects (V_d=0.64cm s^{-1}). The dashed line rectangle indicates the position of the

mean tree crown, i.e. 17 m (mean height of the top) and 5.7 m (mean height of the bottom). The maximum canopy top height recorded in the street is of 29 m.

Figure 10. Concentration contours for CB (left) and CT2 (right) for approaching wind directions (a) WD=60°, (b) WD=240°, (c) WD=180° and (d) WD=330°, with indication of the two hotspots far and close to trees.

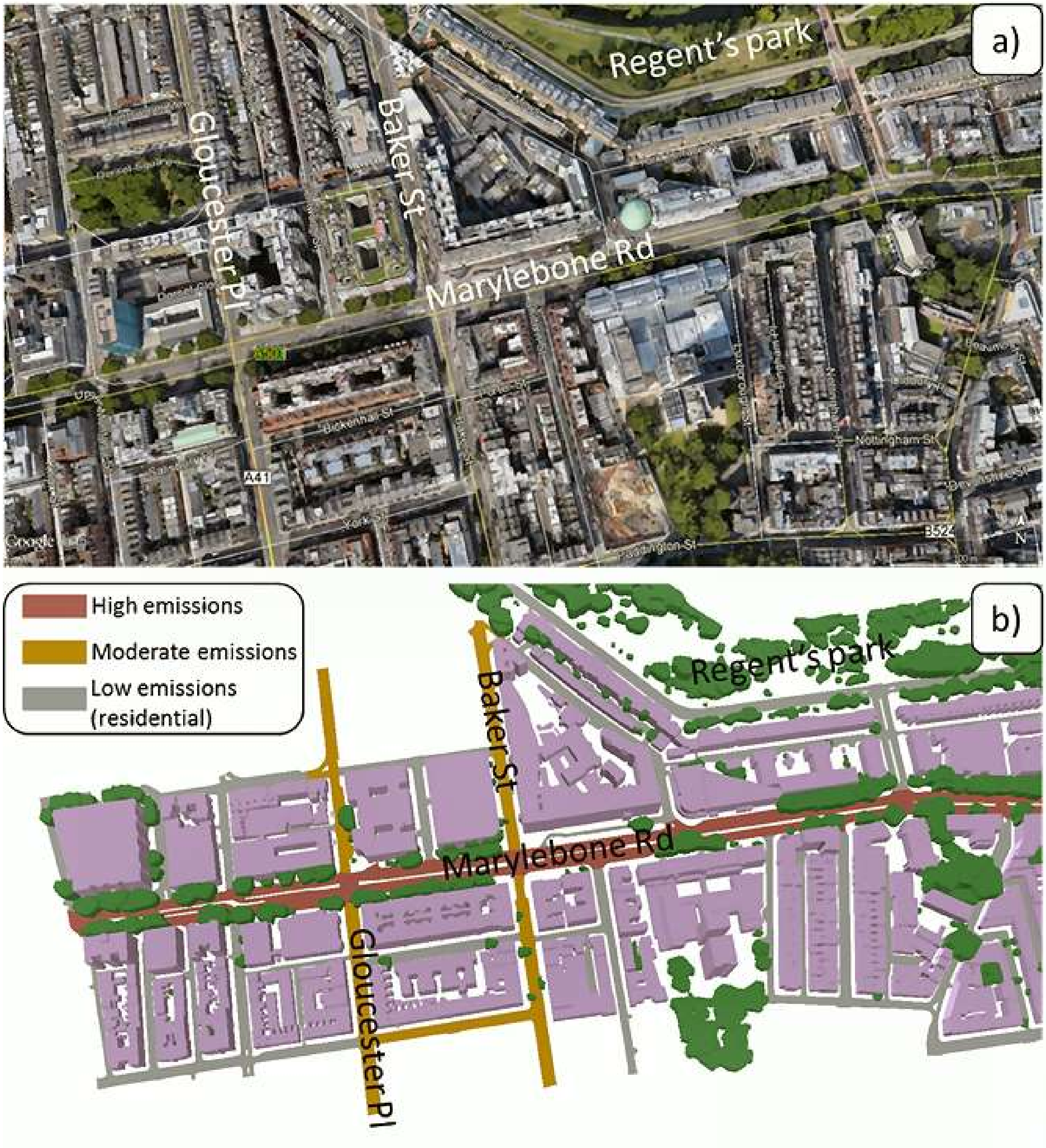
a)
Regent’s park
Gloucester Pl
Baker St
Marylebone Rd
b)
High emissions
Moderate emissions
Low emissions (residential)
Regent’s park
Baker St
Marylebone Rd
Gloucester Pl

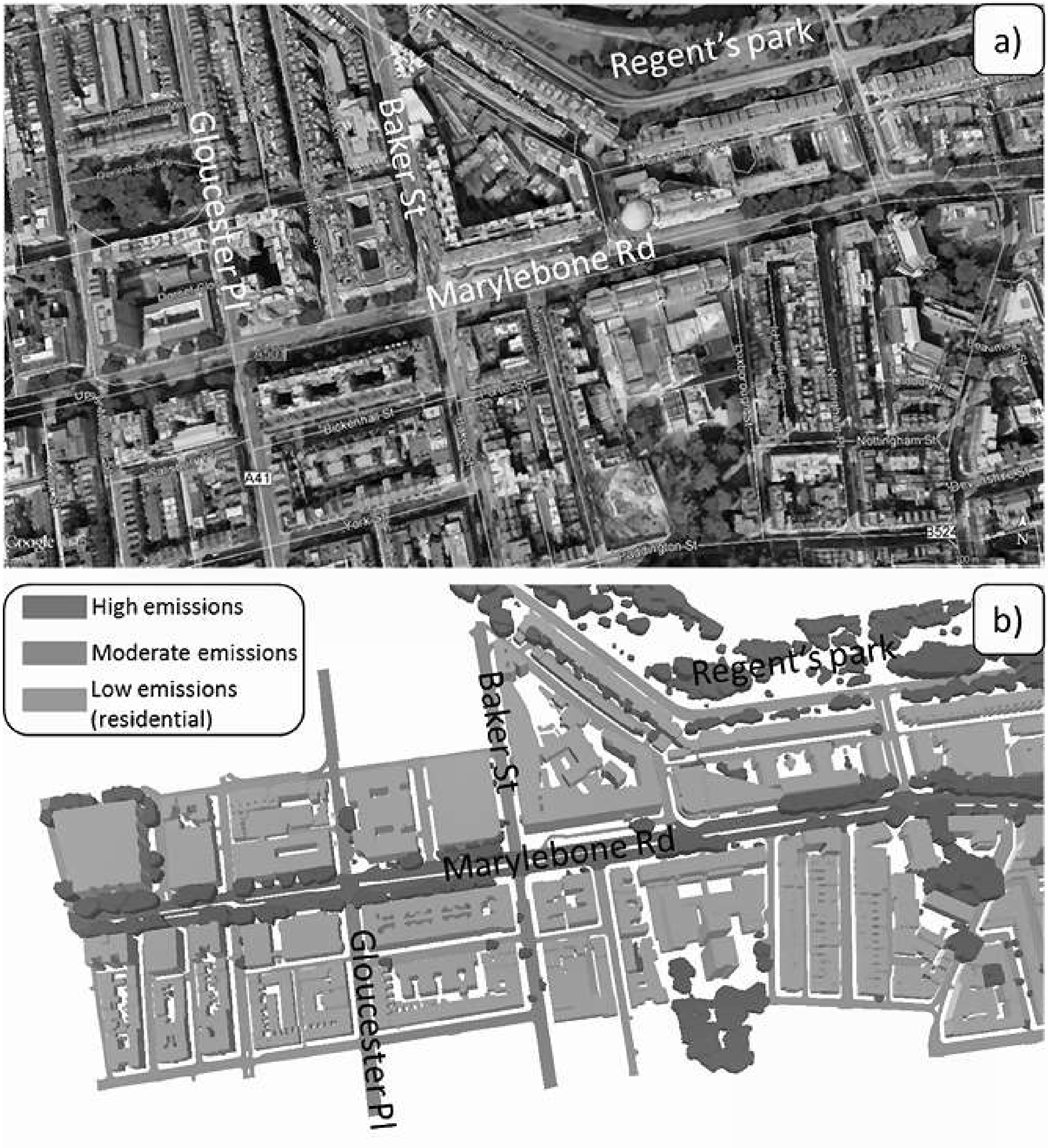

a)
Regent's park
Gloucester Pl
Baker St
Marylebone Rd
b)
High emissions
Moderate emissions
Low emissions (residential)
Regent's park
Baker St
Marylebone Rd
Gloucester Pl

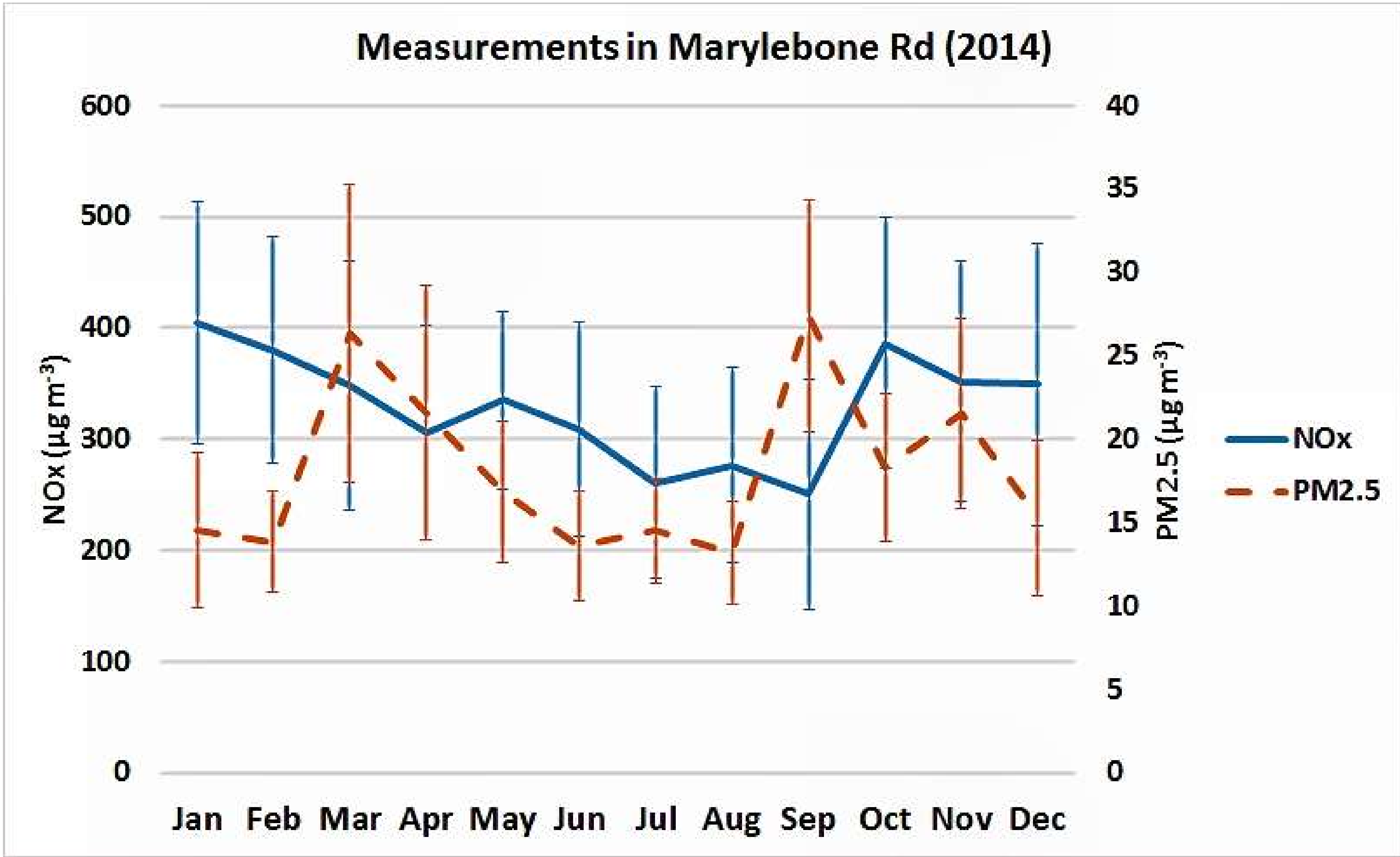

Measurements in Marylebone Rd (2014)
NOx (µg m-3)
PM2.5 (µg m-3)
600
500
400
300
200
100
0
40
35
30
25
20
15
10
5
0
Jan
Feb
Mar
Apr
May
Jun
Jul
Aug
Sep
Oct
Nov
Dec
NOx
PM2.5

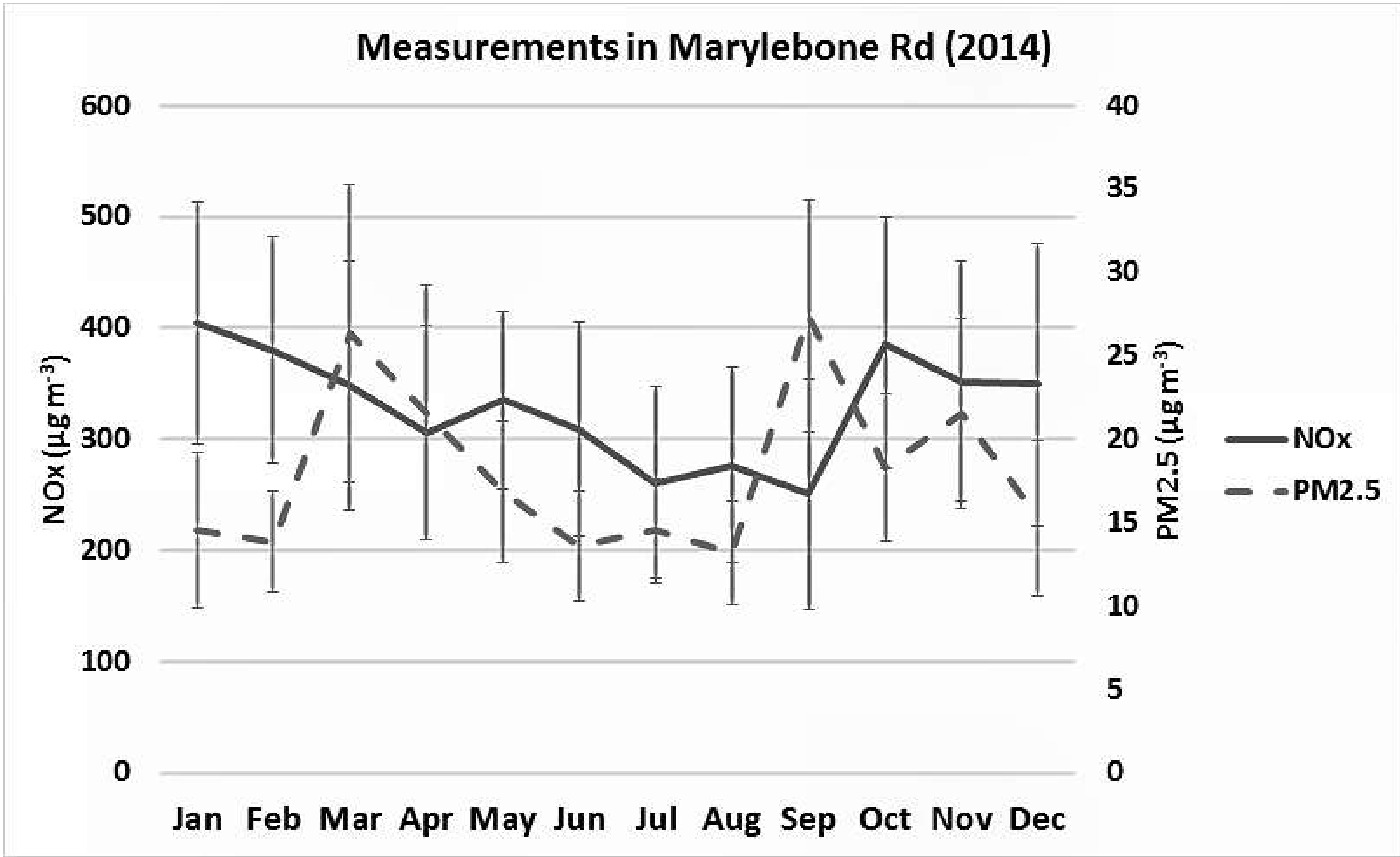
Measurements in Marylebone Rd (2014)
NOx (µg m-3)
PM2.5 (µg m-3)
600
500
400
300
200
100
0
40
35
30
25
20
15
10
5
0
Jan
Feb
Mar
Apr
May
Jun
Jul
Aug
Sep
Oct
Nov
Dec
NOx
PM2.5

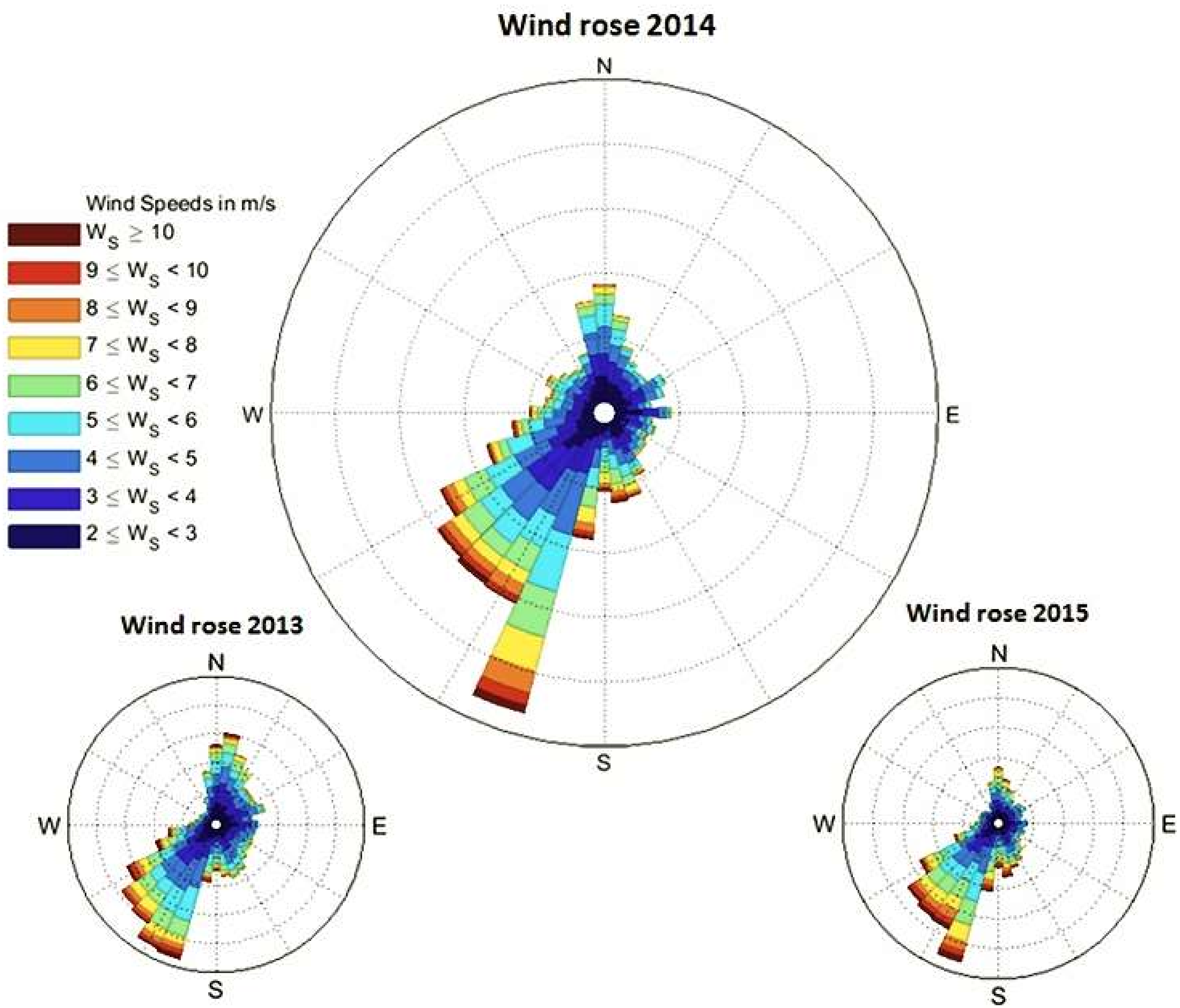
Wind rose 2014
N
E
S
W
Wind Speeds in m/s
$W_S \geq 10$
$9 \leq W_S < 10$
$8 \leq W_S < 9$
$7 \leq W_S < 8$
$6 \leq W_S < 7$
$5 \leq W_S < 6$
$4 \leq W_S < 5$
$3 \leq W_S < 4$
$2 \leq W_S < 3$
Wind rose 2013
Wind rose 2015

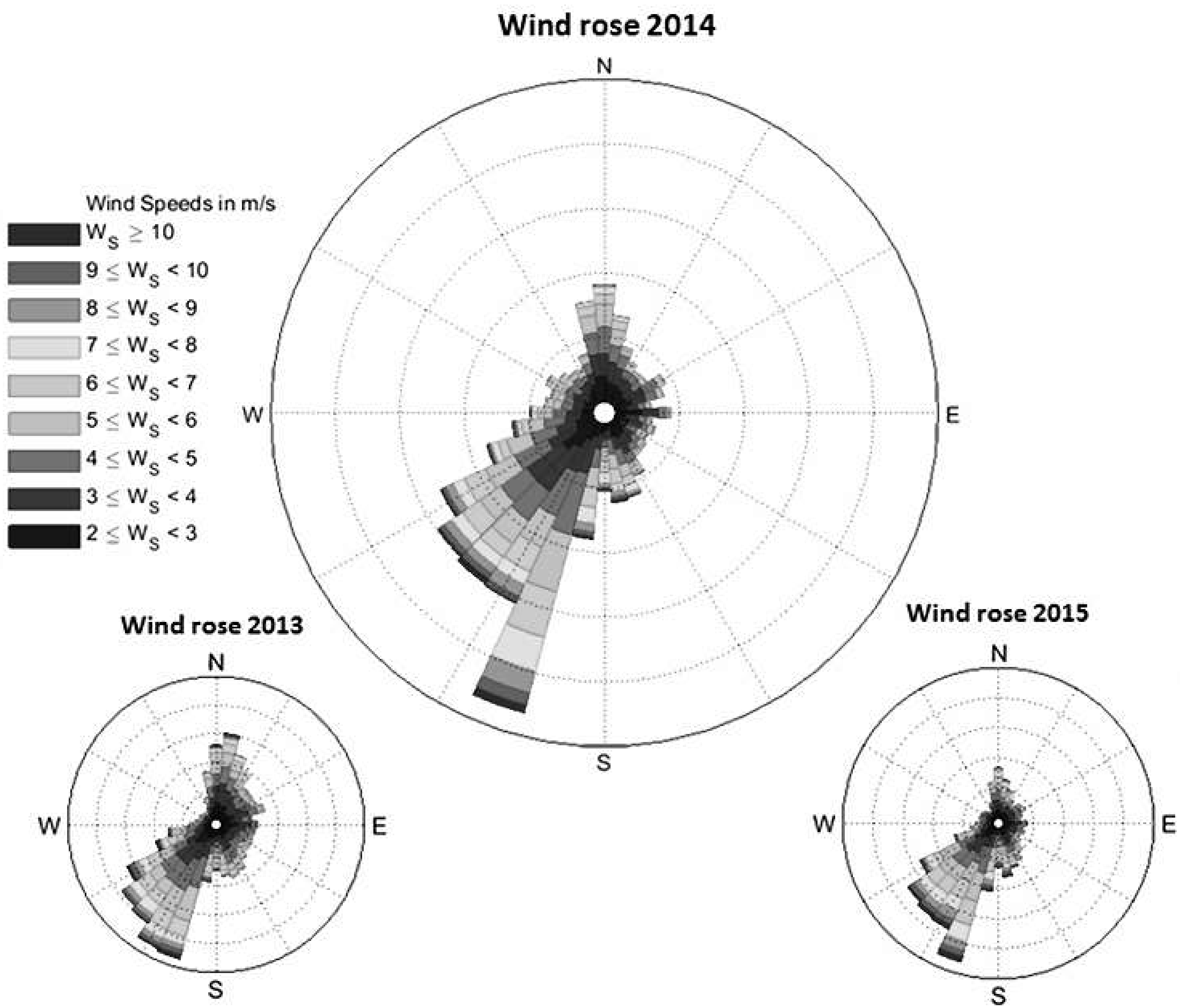
Wind rose 2014
Wind Speeds in m/s
$W_S \geq 10$
$9 \leq W_S < 10$
$8 \leq W_S < 9$
$7 \leq W_S < 8$
$6 \leq W_S < 7$
$5 \leq W_S < 6$
$4 \leq W_S < 5$
$3 \leq W_S < 4$
$2 \leq W_S < 3$
N
E
S
W
Wind rose 2013
Wind rose 2015

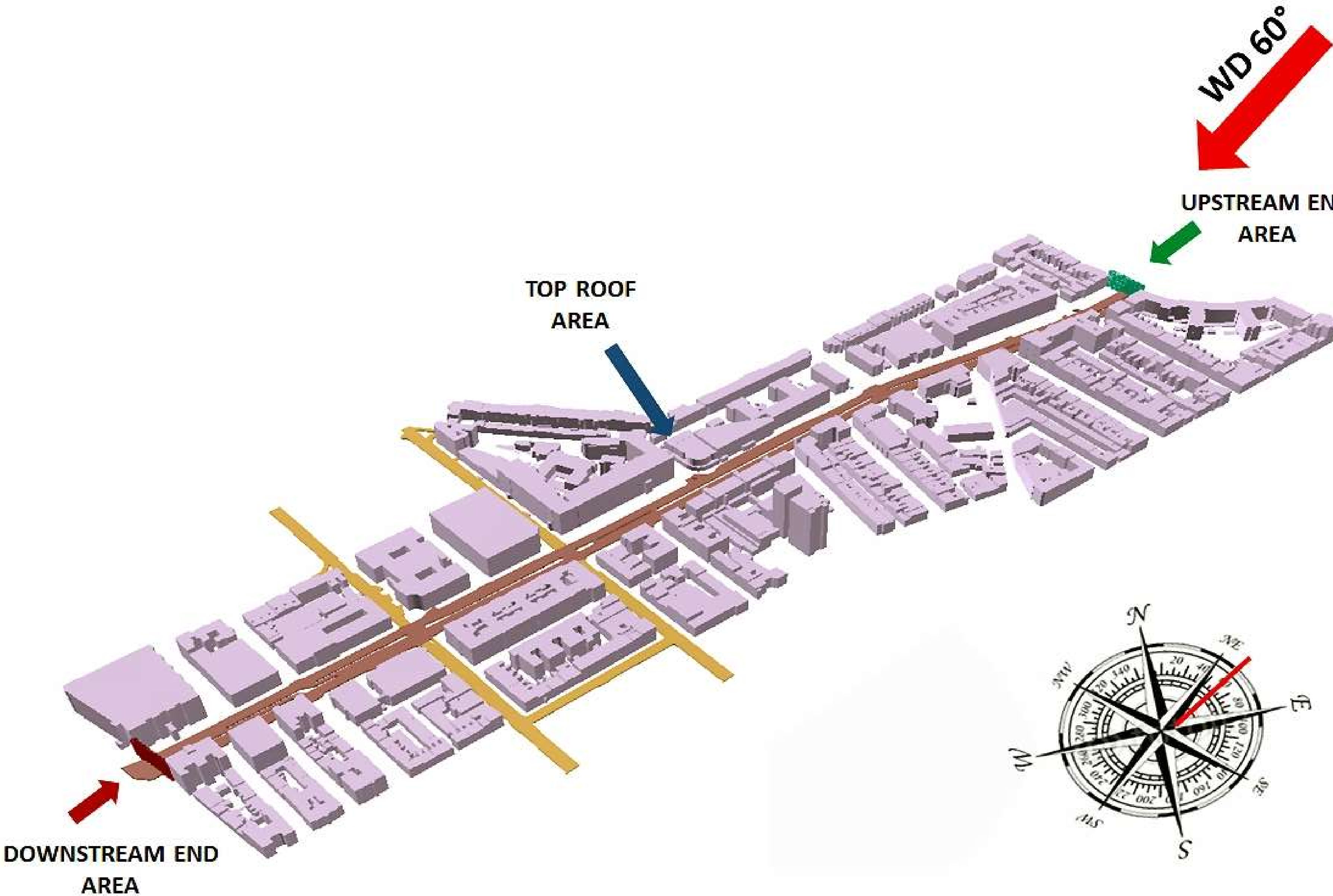
WD 60°
UPSTREAM END
AREA
TOP ROOF
AREA
DOWNSTREAM END
AREA
N
NE
E
SE
S
SW
W
NW

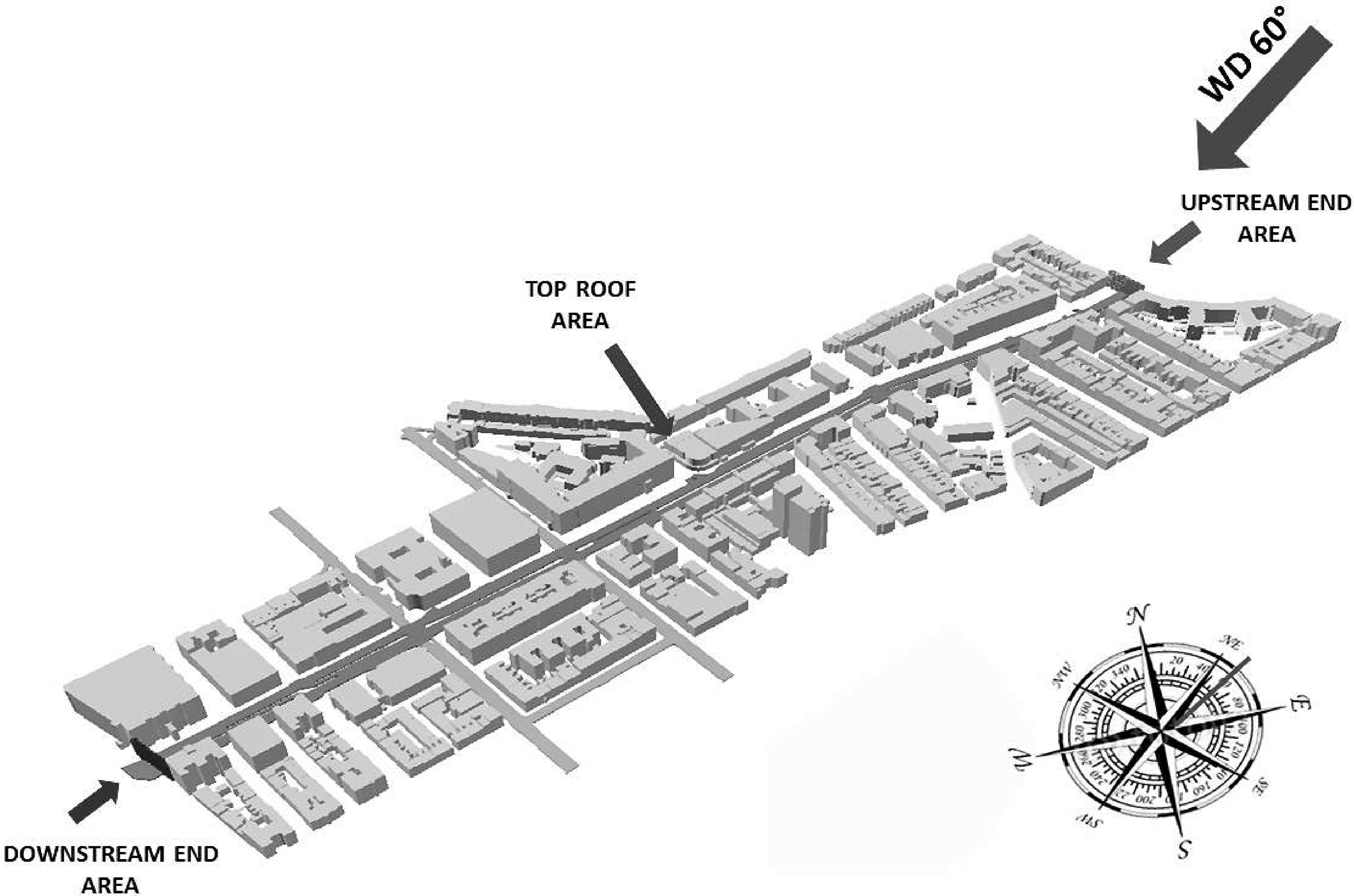
WD 60°
UPSTREAM END AREA
TOP ROOF AREA
DOWNSTREAM END AREA
N
NE
E
SE
S
SW
W
NW

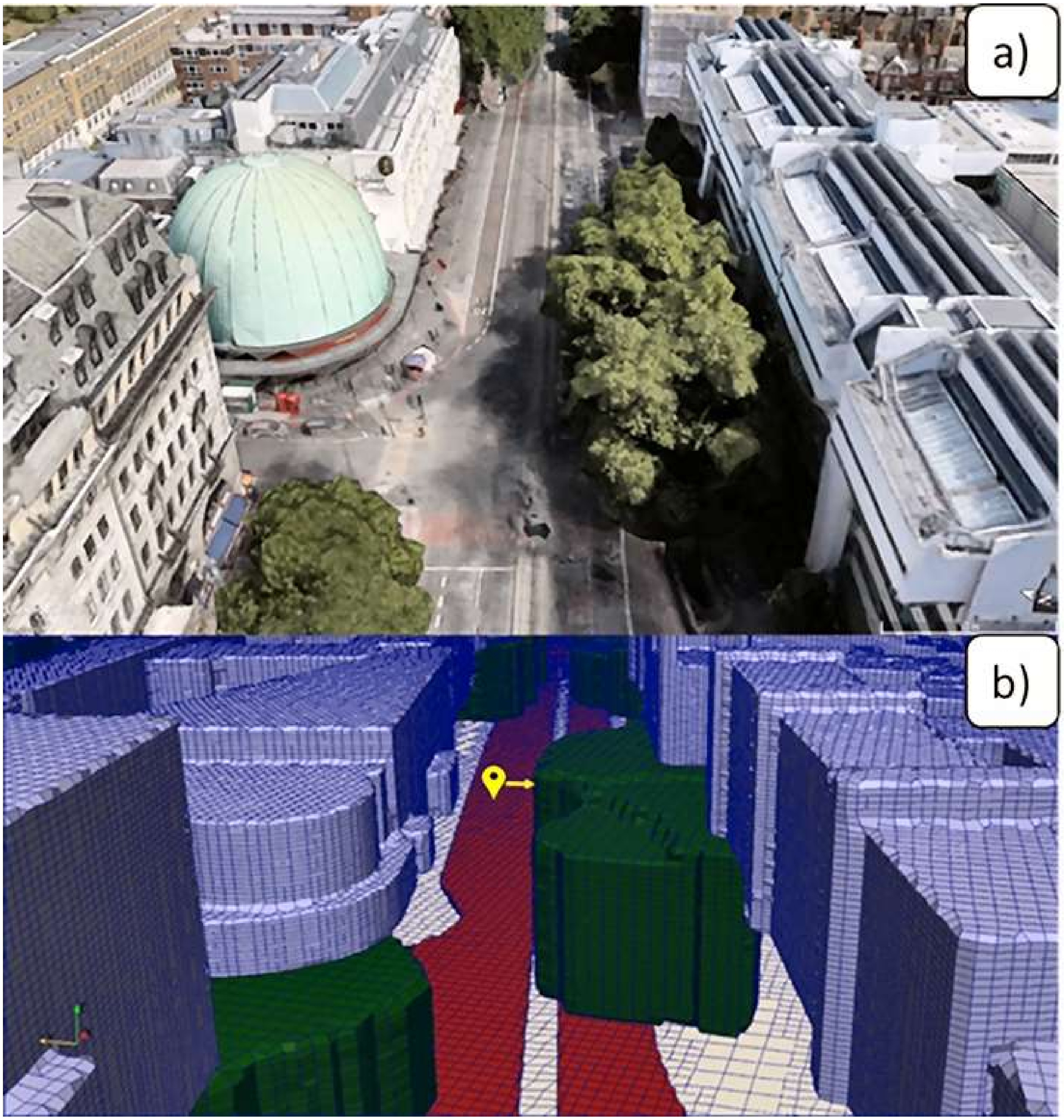
a)
b)

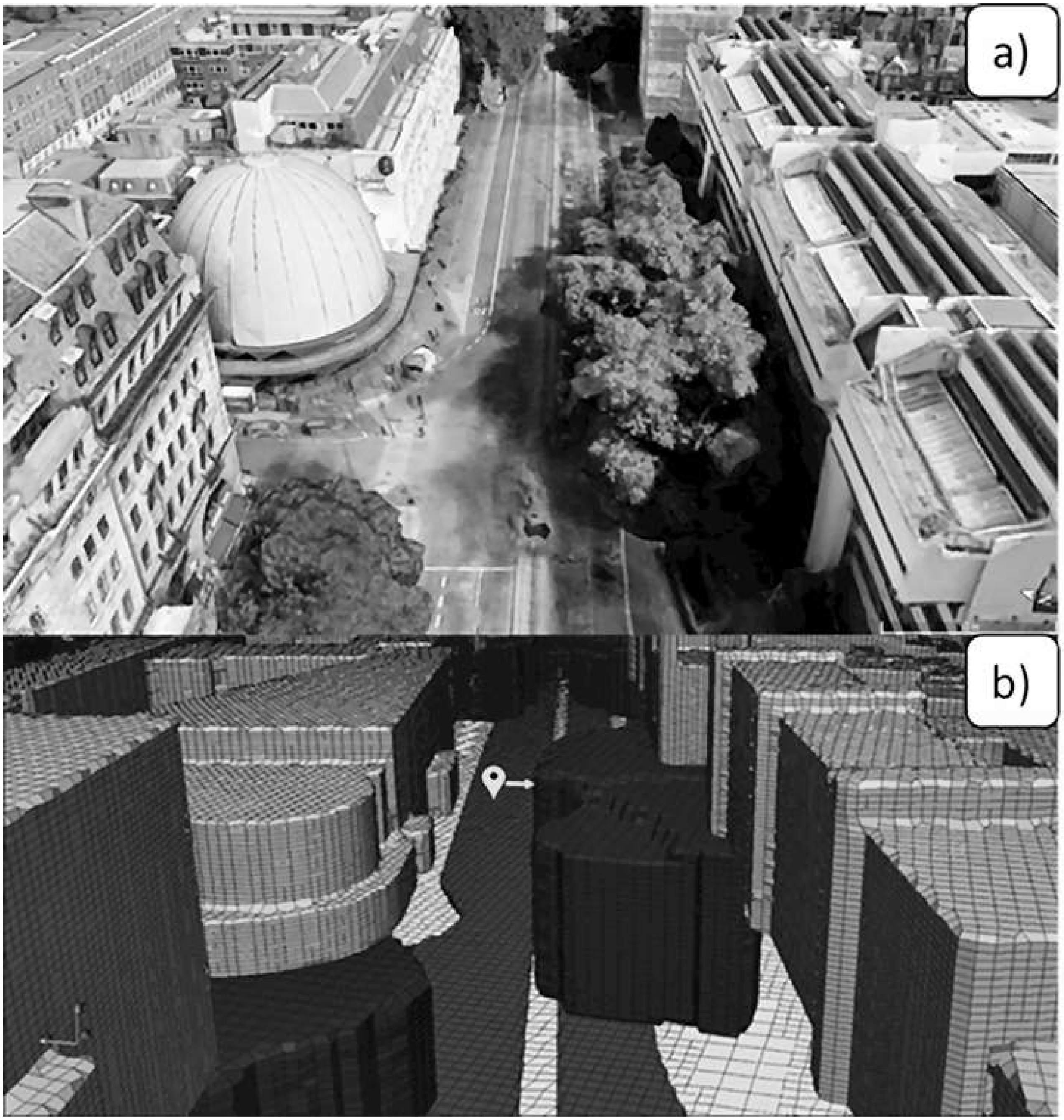
a)
b)

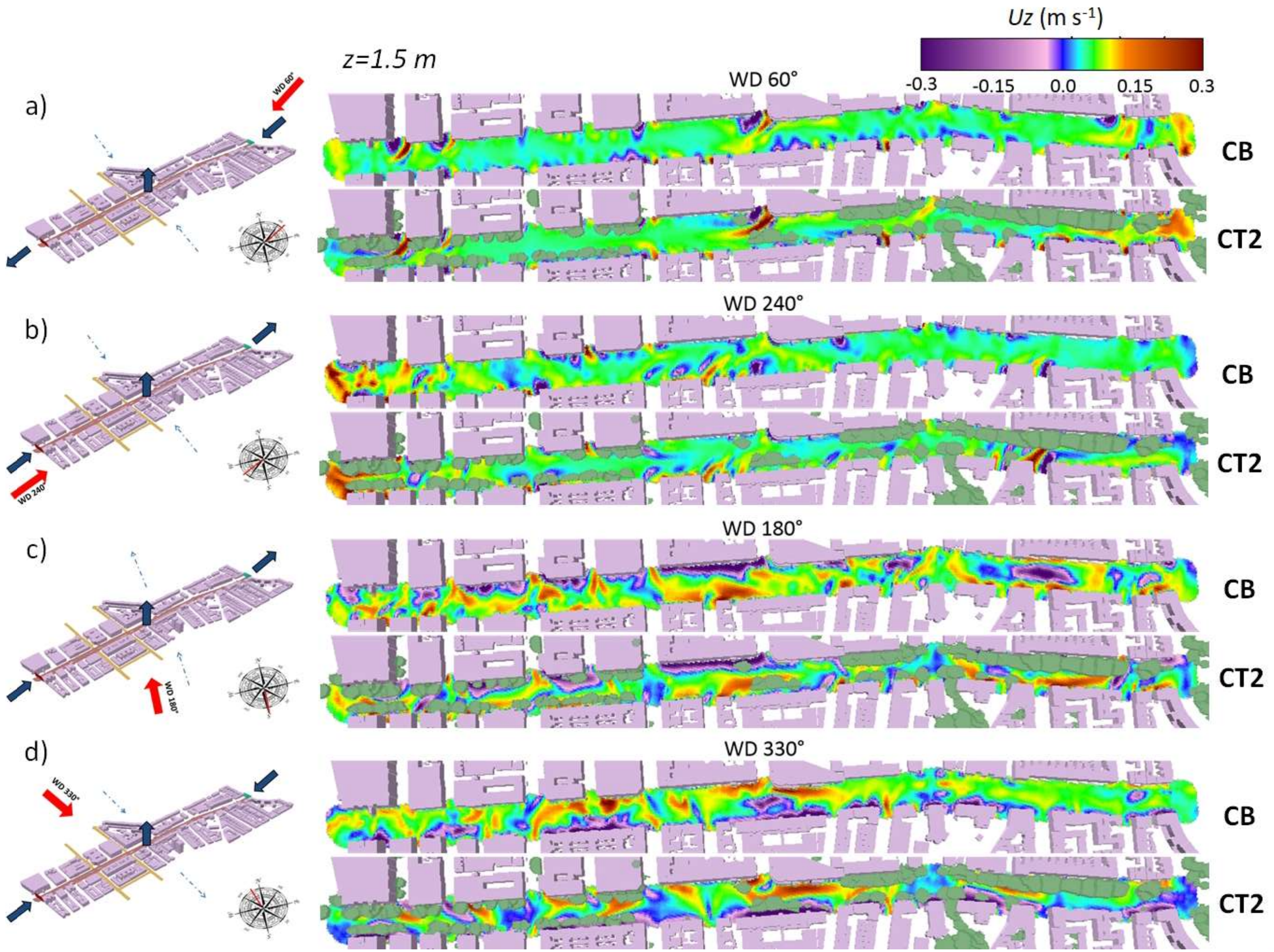

z=1.5 m
Uz (m s-1)
-0.3
-0.15
0.0
0.15
0.3
a)
WD 60°
b)
WD 240°
c)
WD 180°
d)
WD 330°
CB
CT2
CB
CT2
CB
CT2
CB
CT2

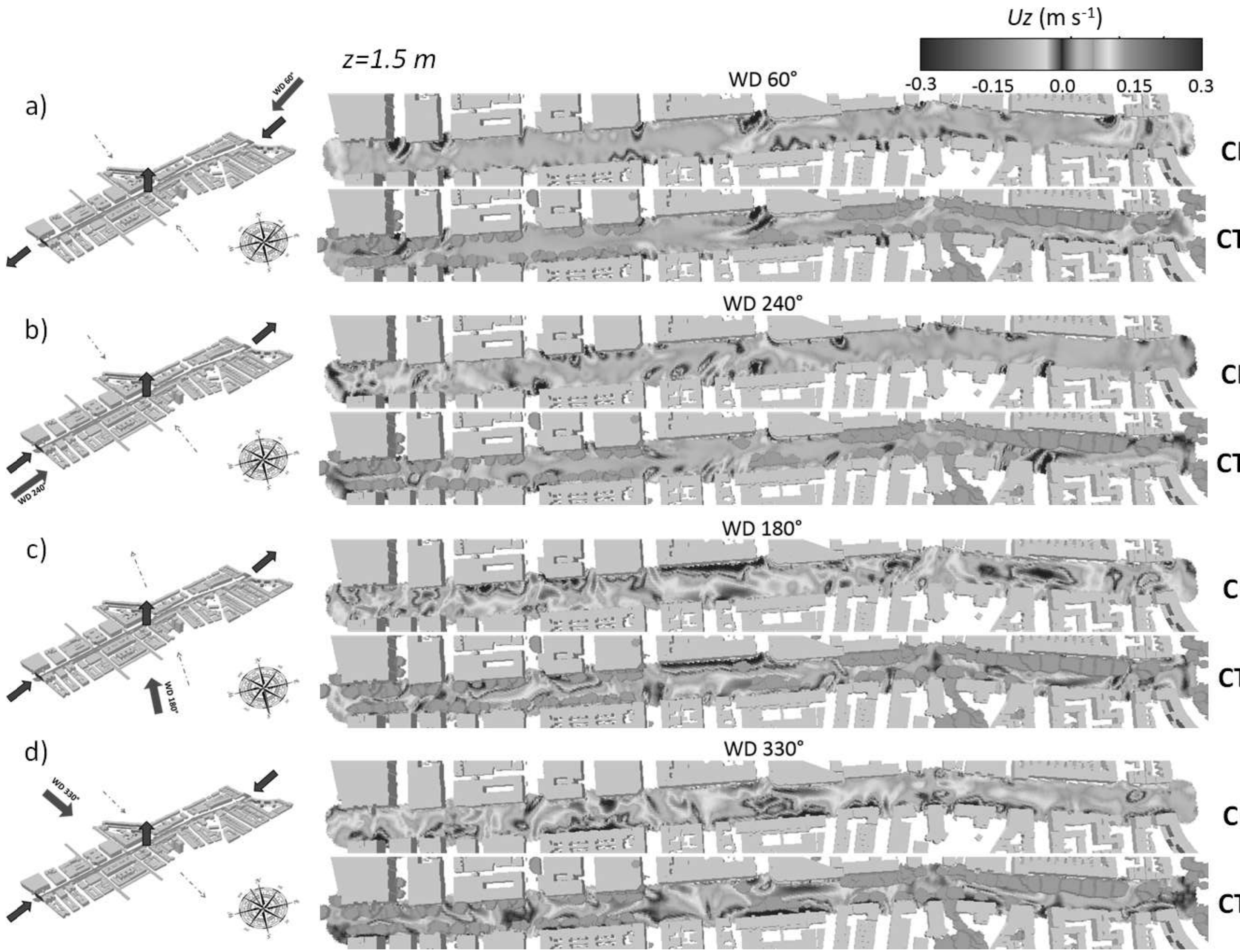
z=1.5 m
Uz (m s-1)
-0.3
-0.15
0.0
0.15
0.3
a)
WD 60°
b)
WD 240°
c)
WD 180°
d)
WD 330°
CB
CT2
CB
CT2
CB
CT2
CB
CT2

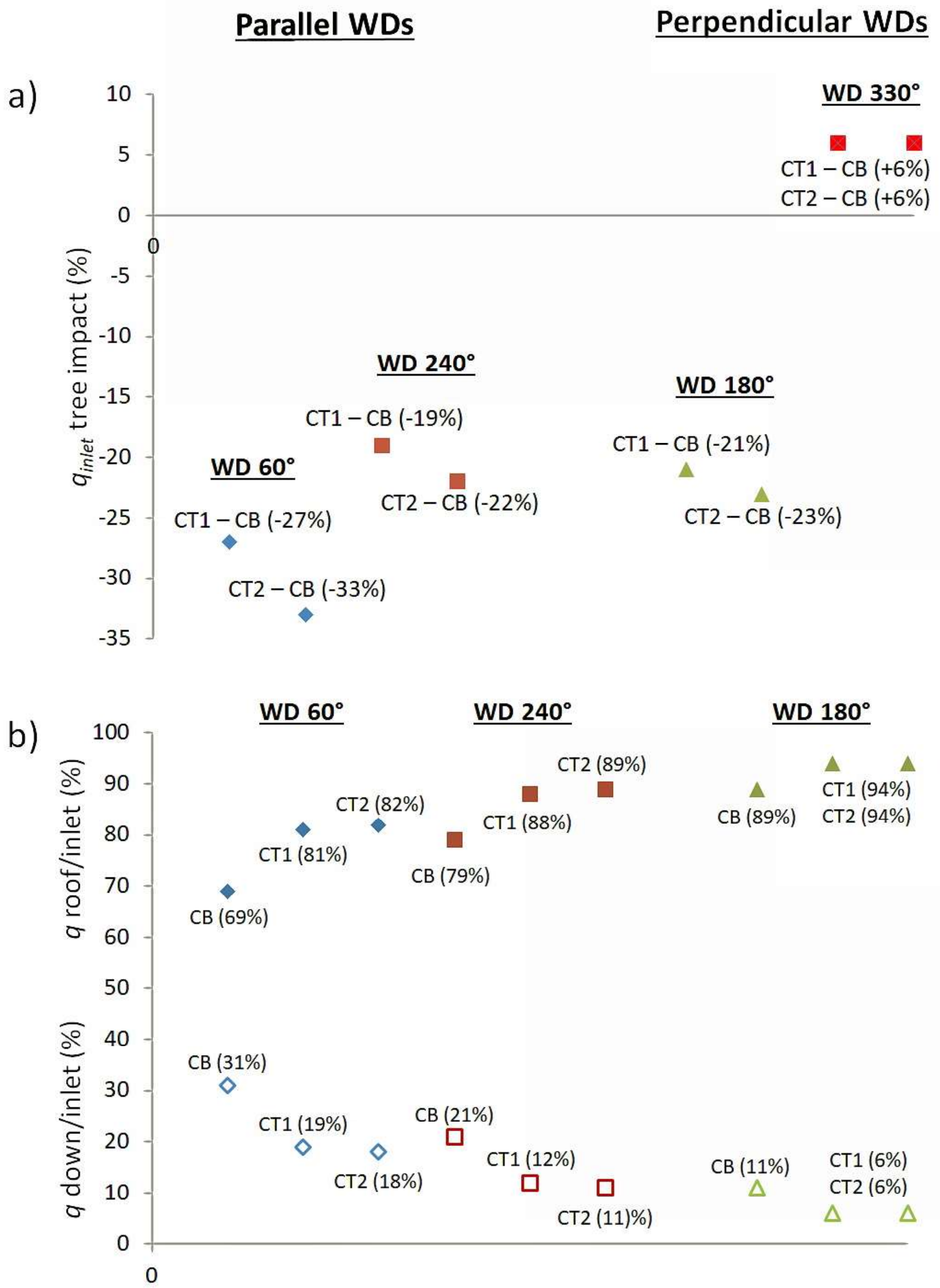

Parallel WDs
Perpendicular WDs
a)
WD 330°
CT1 – CB (+6%)
CT2 – CB (+6%)
WD 240°
CT1 – CB (-19%)
CT2 – CB (-22%)
WD 180°
CT1 – CB (-21%)
CT2 – CB (-23%)
WD 60°
CT1 – CB (-27%)
CT2 – CB (-33%)
q_{inlet} tree impact (%)
10
5
0
-5
-10
-15
-20
-25
-30
-35
0
b)
WD 60°
WD 240°
WD 180°
CT2 (89%)
CT1 (94%)
CT2 (94%)
CT2 (82%)
CT1 (88%)
CB (89%)
CT1 (81%)
CB (79%)
CB (69%)
CB (31%)
CB (21%)
CT1 (19%)
CT1 (12%)
CB (11%)
CT1 (6%)
CT2 (6%)
CT2 (18%)
CT2 (11)%)
q roof/inlet (%)
q down/inlet (%)
100
90
80
70
60
50
40
30
20
10
0
0

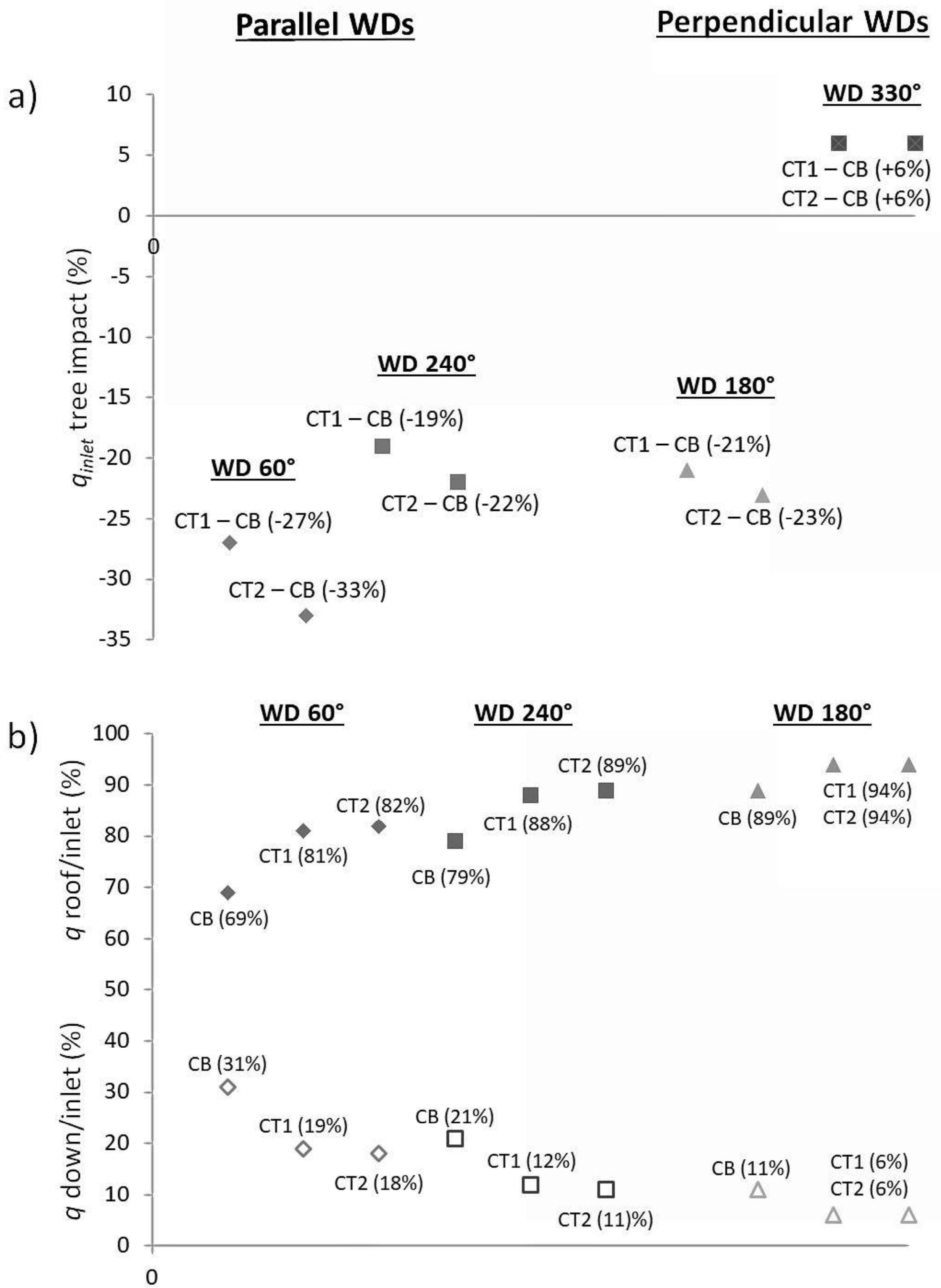
Parallel WDs
Perpendicular WDs
a)
WD 330°
CT1 – CB (+6%)
CT2 – CB (+6%)
q_{inlet} tree impact (%)
WD 240°
CT1 – CB (-19%)
CT2 – CB (-22%)
WD 180°
CT1 – CB (-21%)
CT2 – CB (-23%)
WD 60°
CT1 – CB (-27%)
CT2 – CB (-33%)
b)
WD 60°
WD 240°
WD 180°
q roof/inlet (%)
q down/inlet (%)
CT2 (89%)
CT2 (82%)
CT1 (88%)
CB (89%)
CT1 (94%)
CT2 (94%)
CT1 (81%)
CB (79%)
CB (69%)
CB (31%)
CT1 (19%)
CB (21%)
CT2 (18%)
CT1 (12%)
CB (11%)
CT1 (6%)
CT2 (6%)
CT2 (11)%)

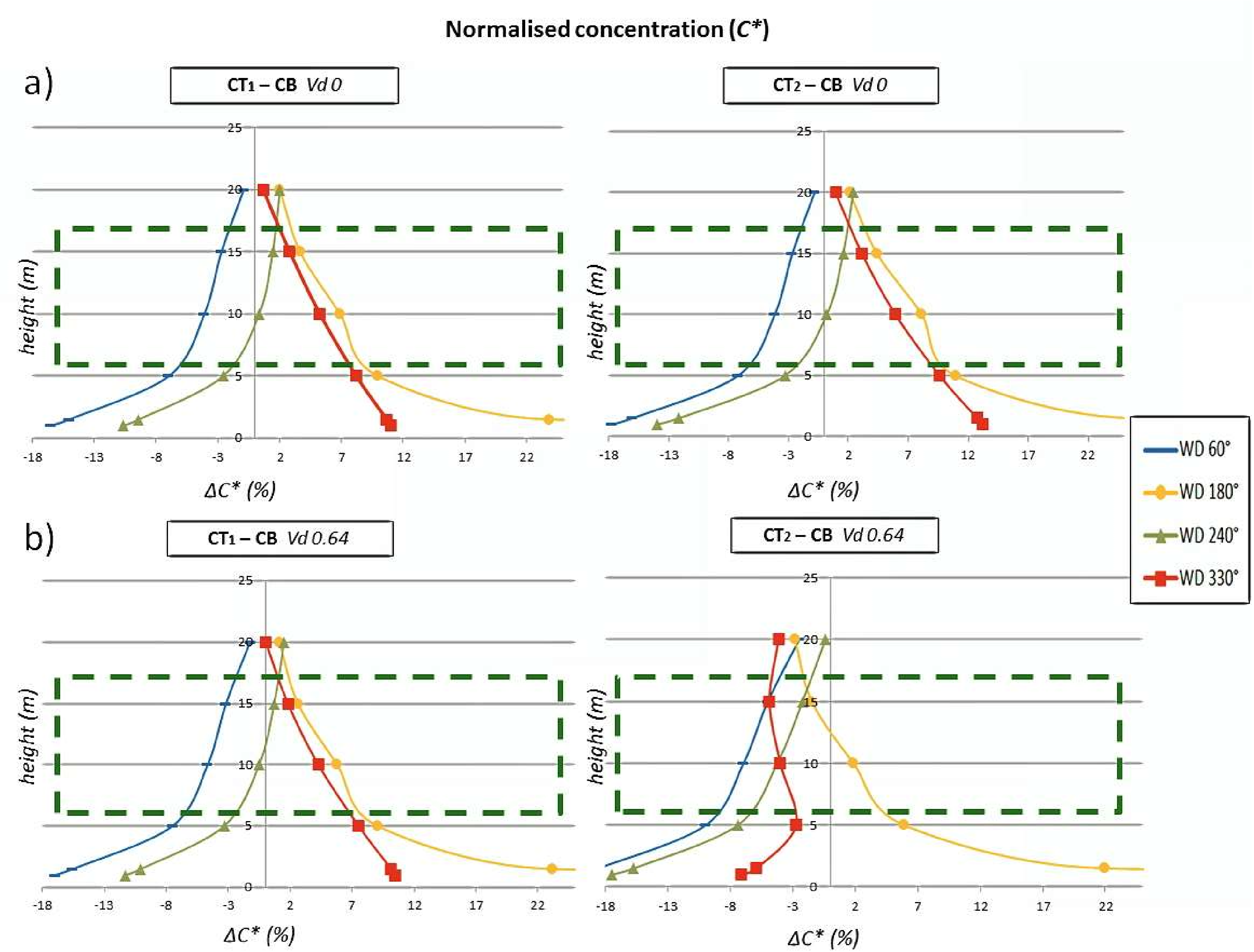

Normalised concentration (C*)
a)
CT1 – CB Vd 0
CT2 – CB Vd 0
b)
CT1 – CB Vd 0.64
CT2 – CB Vd 0.64
height (m)
ΔC* (%)
WD 60°
WD 180°
WD 240°
WD 330°

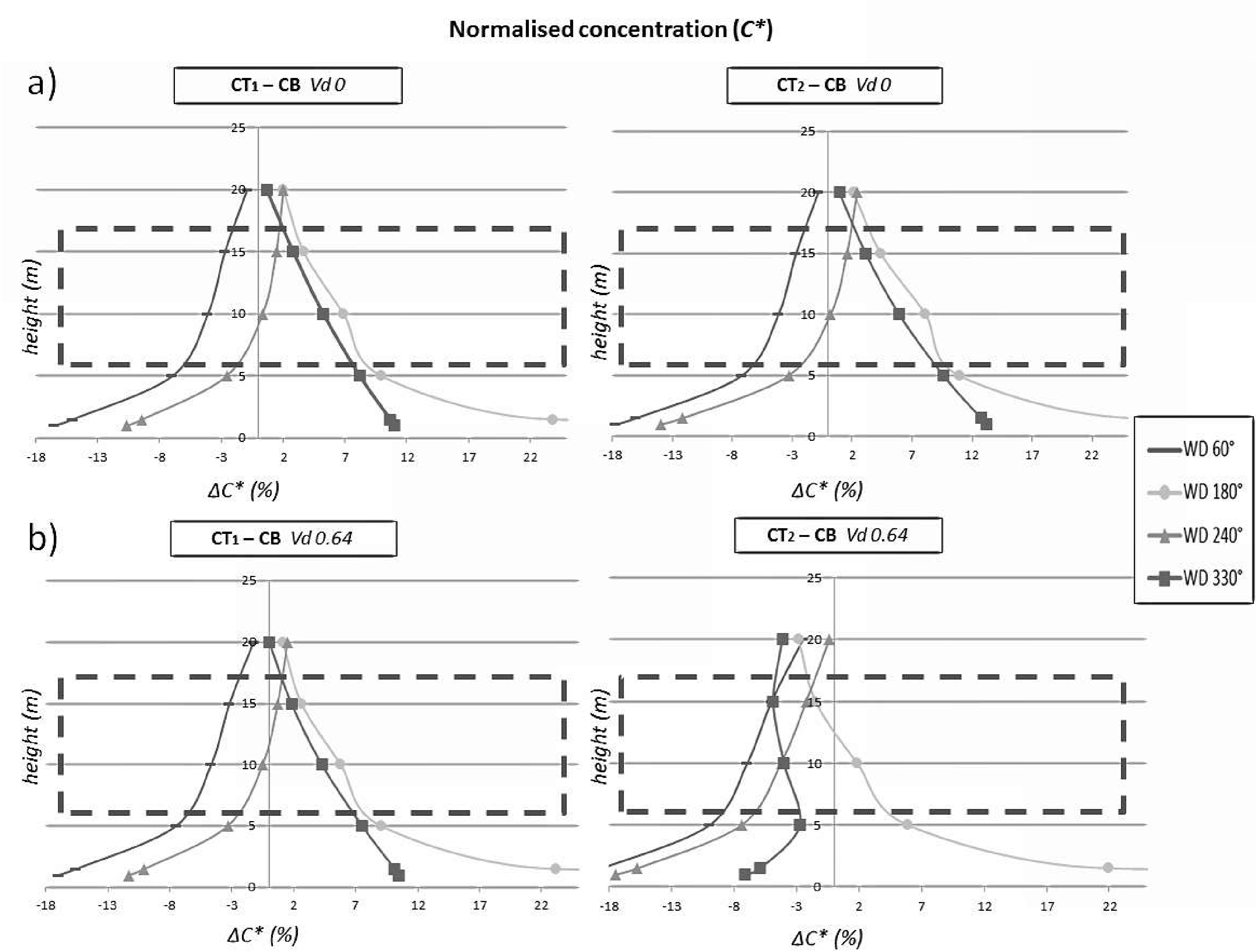

Normalised concentration (C*)
a)
CT1 – CB Vd 0
CT2 – CB Vd 0
b)
CT1 – CB Vd 0.64
CT2 – CB Vd 0.64
height (m)
ΔC* (%)
25
20
15
10
5
0
-18
-13
-8
-3
2
7
12
17
22
WD 60°
WD 180°
WD 240°
WD 330°

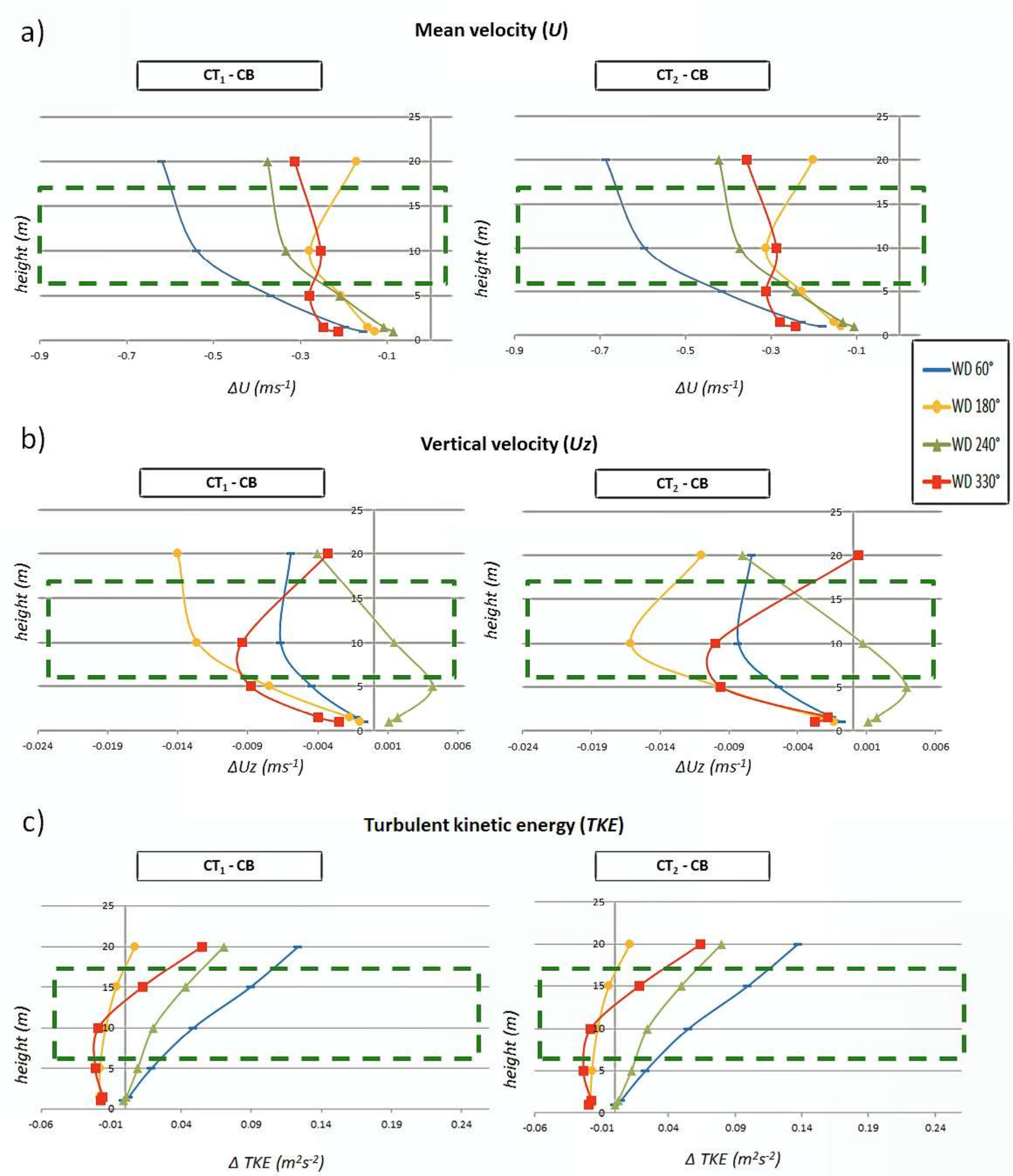
a)
Mean velocity (U)
CT1 - CB
CT2 - CB
height (m)
ΔU (ms-1)
WD 60°
WD 180°
WD 240°
WD 330°
b)
Vertical velocity (Uz)
CT1 - CB
CT2 - CB
height (m)
ΔUz (ms-1)
c)
Turbulent kinetic energy (TKE)
CT1 - CB
CT2 - CB
height (m)
Δ TKE (m2s-2)

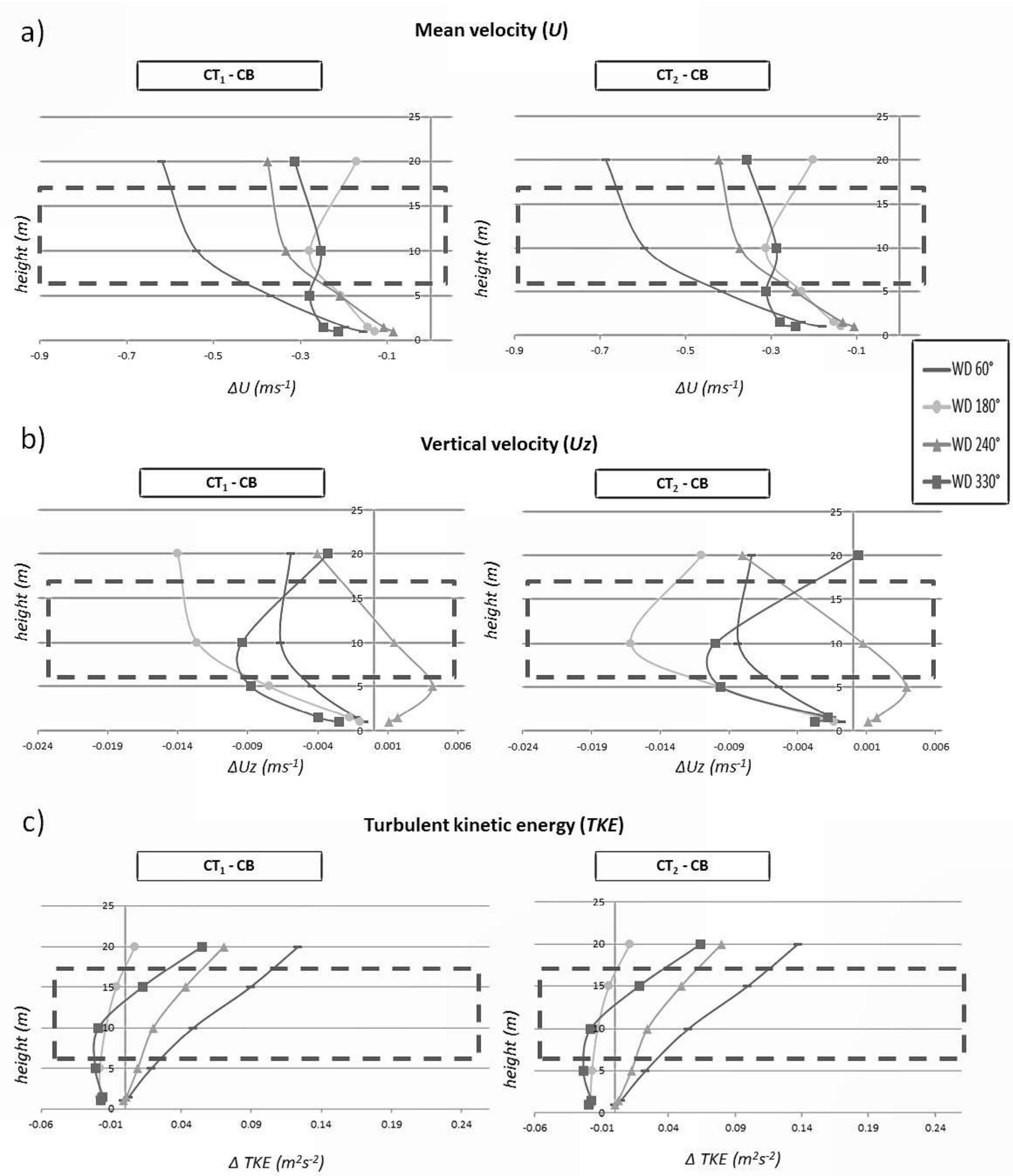

a)
Mean velocity (U)
CT1 - CB
CT2 - CB
height (m)
25
20
15
10
5
0
-0.9
-0.7
-0.5
-0.3
-0.1
ΔU (ms-1)
WD 60°
WD 180°
WD 240°
WD 330°
b)
Vertical velocity (Uz)
CT1 - CB
CT2 - CB
height (m)
-0.024
-0.019
-0.014
-0.009
-0.004
0.001
0.006
ΔUz (ms-1)
c)
Turbulent kinetic energy (TKE)
CT1 - CB
CT2 - CB
height (m)
-0.06
-0.01
0.04
0.09
0.14
0.19
0.24
Δ TKE (m2s-2)

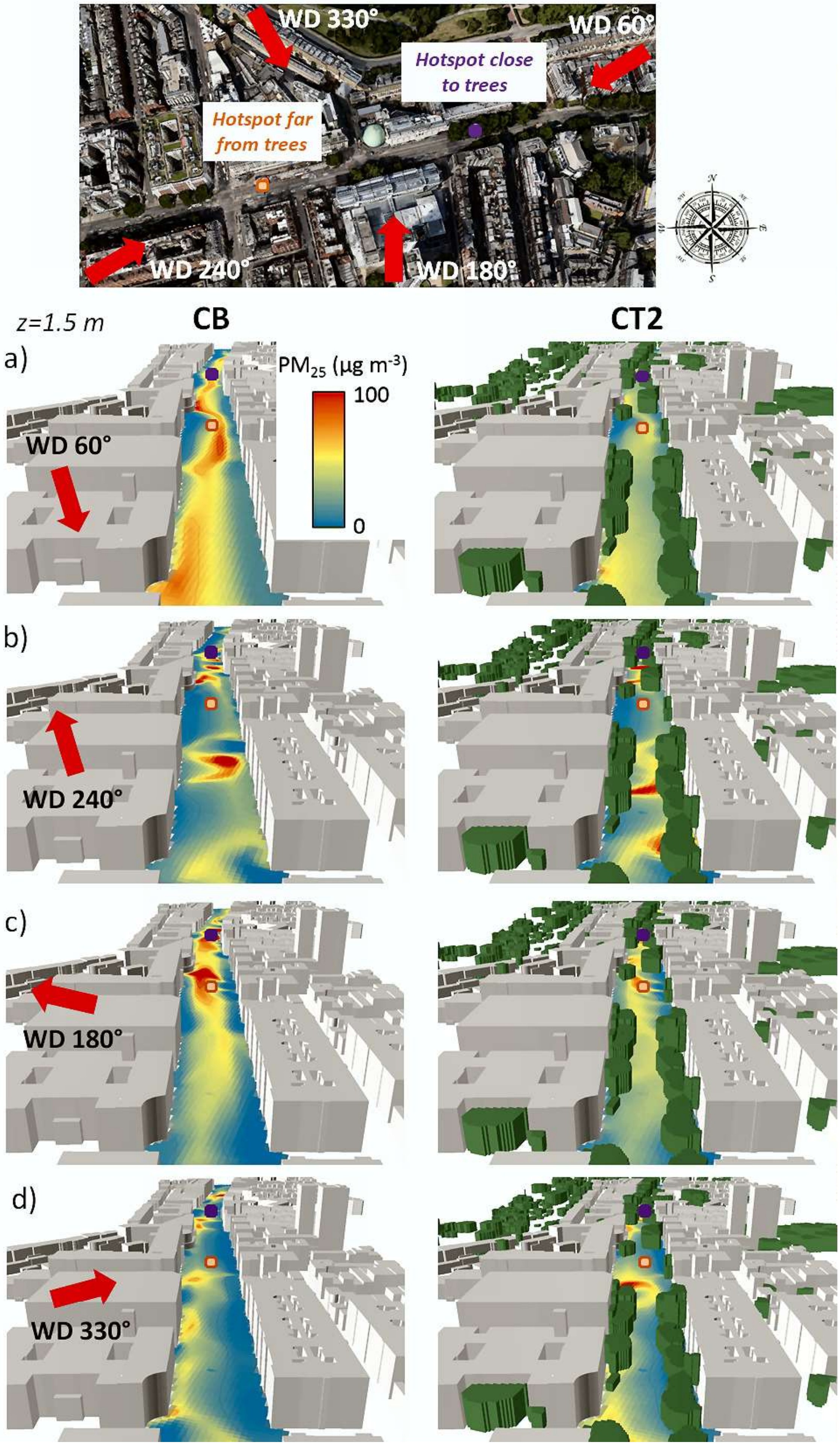

WD 330°
WD 60°
Hotspot close to trees
Hotspot far from trees
WD 240°
WD 180°
z=1.5 m
CB
CT2
a)
PM25 (µg m-3)
100
0
WD 60°
b)
WD 240°
c)
WD 180°
d)
WD 330°

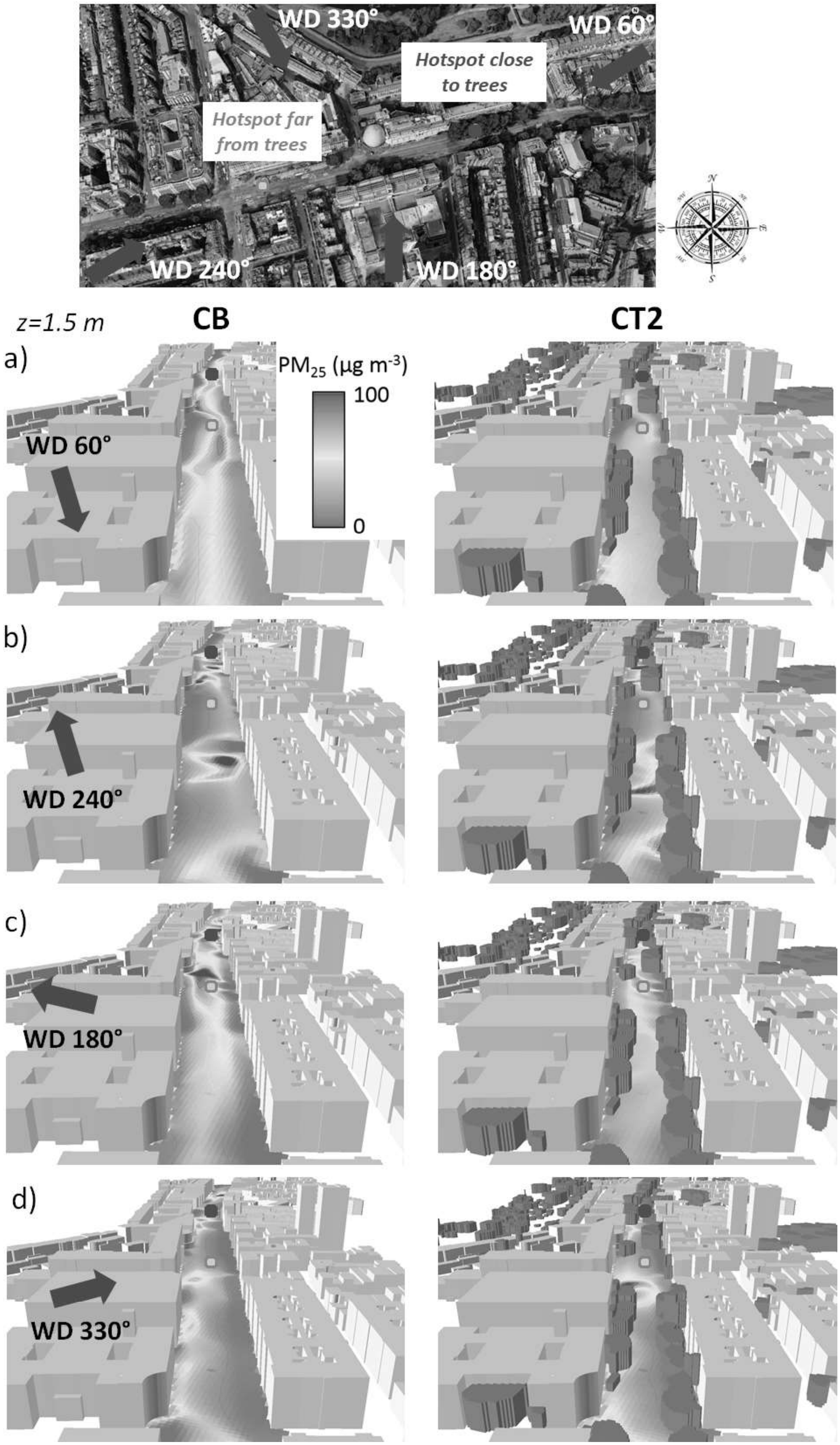
WD 330°
WD 60°
Hotspot close to trees
Hotspot far from trees
WD 240°
WD 180°
z=1.5 m
CB
CT2
a)
PM25 (µg m-3)
100
0
WD 60°
b)
WD 240°
c)
WD 180°
d)
WD 330°

Table 1. NO_x and $PM_{2.5}$ emissions estimated from Annual Average Daily Flows (adapted from Jeanjean et al., 2017).

	Marylebone Rd	**A41 - Gloucester Place**	**A41 - Baker Street**
Annual Average Daily Flows (AADF)	79078	14579	12198
Average NO_x emission (mg m^{-1} s^{-1})	0.68	0.11	0.10
Average $PM_{2.5}$ emission (mg m^{-1} s^{-1})	0.031	0.006	0.005

Table 2. Cases investigated with different types of trees, seasons and meteorological data simulated with the OpenFOAM CFD software platform.

Name	**Trees**	**Typical season**	**LAD (m^2 m^{-3})**	**Wind speed (m s^{-1})**	**Wind direction (°)**
CB (Case of Buildings only)	Leaf-free	Winter	0	3 5	Parallel: 60, 240 Perpendicular: 180, 330
CT1 (Case of Trees 1)	Half-grown leaves	Spring & Autumn	1.06		
CT2 (Case of Trees 2)	Fully grown leaves	Summer	1.6		

Table 3. Flow rates for all the cases investigated with a wind speed of 3 m s^{-1}. WD stands for wind direction.

Flow rate *q* (m^3/s)	**Parallel WDs**		**Perpendicular WDs**	
	WD 60°	**WD 240°**	**WD 180°**	**WD 330°**
CB				
East end	1497	*-1007*	*-485*	81
West end	*-1016*	1556	622	409
Top roof	*-2270*	*-3859*	*-3772*	*-2127*
Buildings empty spaces	1790	3309	3635	1637
CT1				
East end	973	*-478*	*-200*	40
West end	*-453*	1073	450	147
Top roof	*-1946*	*-3448*	*-3148*	*-2260*
Buildings empty spaces	1427	2853	2897	2073
CT2				
East end	887	*-430*	*-198*	34
West end	*-397*	984	432	128
Top roof	*-1819*	*-3366*	*-3097*	*-2257*
Buildings empty spaces	1329	2812	2864	2095

Table 4. Spatially-averaged $PM_{2.5}$ pollutant fluxes at street openings (with no deposition) due to mean flow (*FAm*) and turbulent fluctuations (*FAt*) for all the cases investigated with a wind speed of 3 m s^{-1}. WD stands for wind direction.

Pollutant fluxes (mg s^{-1})	**Parallel WDs**				**Perpendicular WDs**			
	WD 60°		**WD 240°**		**WD 180°**		**WD 330°**	
	FAm	***FAt***	***FAm***	***FAt***	***FAm***	***FAt***	***FAm***	***FAt***
CB								
East end	0.1	0.0	-5.6	0.0	-1.1	0.0	0.0	0.0
West end	-6.6	-0.2	0.2	0.0	0.1	0.0	0.0	0.0
Top roof	14.7	24.3	23.4	18.9	21.8	8.5	7.1	5.7
CT1								
East end	0.2	0.0	-3.3	0.0	-0.5	0.0	0.0	0.0
West end	-2.2	-0.2	0.2	0.0	0.1	0.0	0.3	0.2
Top roof	12.0	34.6	26.0	29.8	20.7	10.4	8.6	18.0
CT2								
East end	0.2	0.0	-2.9	0.0	-0.6	0.0	0.1	0.0
West end	-1.9	-0.1	0.2	0.0	0.1	0.0	0.3	0.2
Top roof	11.2	35.5	25.6	30.2	19.7	11.2	9.1	20.5

Table 45. Horizontally-averaged *ΔC** for tree *vs* tree-free cases under wind speed of 3 m s^{-1} and four wind directions (WD=60°, WD=180°, WD=240°, WD=330°) within the whole Marylebone Rd (see Fig. 8). Mean: averaged value over all the heights of the street; Ped: value at z=1.5m; Top: value at z=20m.

$\Delta C^* = [(CT_1 - CB)/C_0] \times 100$ (%)						
	Aerodynamic effects (*Vd 0*)			**Aerodynamic + Deposition effects (*Vd 0.64*)**		
WD	**Mean**	**Ped**	**Top**	**Mean**	**Ped**	**Top**
60°	-8	-15	-1	-8	-16	-1
240°	-3	-9	2	-4	-10	1
180°	32	24	2	31	23	1
330°	6	11	1	6	10	0
$\Delta C^* = [(CT_2 - CB)/C_0] \times 100$ (%)						
	Aerodynamic effects (*Vd 0*)			**Aerodynamic + Deposition effects (*Vd 0.64*)**		
WD	**Mean**	**Ped**	**Top**	**Mean**	**Ped**	**Top**
60°	-8	-16	-1	-11	-19	-2
240°	-4	-12	2	-8	-16	-0.4
180°	36	26	2	31	22	-3
330°	8	13	1	-5	-6	-4

Table ~~5~~6. ΔC^* for tree (CT2) *vs* tree-free cases under wind speed of 3 m s^{-1} and four wind directions (WD=60°, WD=180°, WD=240°, WD=330°) at one hotspot far and one hotspot close to trees (see Fig. 10). Mean: averaged value over all the heights of the street; Ped: value at z=1.5m; Top: value at z=20m.

$\Delta C^* = [(CT_2 - CB)/C_0] \times 100$ (%) *(hotspot far from trees)*						
	Aerodynamic effects (*Vd 0*)			**Aerodynamic + Deposition effects (*Vd 0.64*)**		
WD	**Mean**	**Ped**	**Top**	**Mean**	**Ped**	**Top**
60°	-18	-38	-3	-19	-39	-3
240°	-9	-19	-1	-11	-21	-3
180°	10	4	0.5	10	3	-0.1
330°	47	61	20	39	42	6
$\Delta C^* = [(CT_2 - CB)/C_0] \times 100$ (%) *(hotspot close to trees)*						
	Aerodynamic effects (*Vd 0*)			**Aerodynamic + Deposition effects (*Vd 0.64*)**		
WD	**Mean**	**Ped**	**Top**	**Mean**	**Ped**	**Top**
60°	-13	-23	-0.4	-16	-27	-3
240°	-9	-33	6	-14	-38	4

180°	108	-94	52	66	-118	8
330°	7	12	1	-3	-1	-5